Materials Science of the Earth's Interior, edited by I. Sunagawa, pp. 545–583.

HYDROTHERMAL SYNTHESIS AND PHASE RELATIONS OF THE POLYMETALLIC SULFIDE SYSTEM, ESPECIALLY ON THE Cu–Fe–Bi–S SYSTEM

Asahiko SUGAKI, Arashi KITAKAZE, and Kenichiro HAYASHI

Institute of Mineralogy, Petrology, and Economic Geology, Faculty of Science, Tohoku University, Sendai, Japan

1. *Introduction*

Metallic sulfide and sulfosalt minerals are very important as ore minerals and, in many cases, they occur from a hydrothermal solution. It is a very interesting geological problem in making clear the forming process and condition of them in nature. Experimental studies of hydrothermal synthesis and phase equilibrium of sulfide minerals are significant in order to know their forming conditions, and have been carried out over the past 20 years by several authors.

BRYSTOV and KUZ'MINA (1959) produced galena and sphalerite from a powder of simple sulfide in an aqueous solution of lithium and sodium chlorides at 350° and 450°C. KUZ'MINA (1961) and IKORNIKOVA (1962) found that an aqueous solution of ammonium chloride was the best solvent for the synthesis of galena and sphalerite. LAUDISE *et al.* (1965) succeeded in synthesizing large crystals of sphalerite using a potassium hydroxide aqueous solution at 350°C. The synthetic method employed by them was that of thermal gradient transportation using a difference of solubility due to temperature. BARNARD and CHRISTOPHER (1966) first synthesized the ternary sulfide minerals, chalcopyrite $CuFeS_2$, in a sodium chloride aqueous solution *in situ*. CHERNYSHEV *et al.* (1968) performed the hydrothermal synthesis of sphalerite, pyrrhotite, and pyrite of the system Fe–Zn–S in an ammonium chloride solution at temperatures from 250° to 500°C and obtained the solvus of the sphalerite solid solution for pyrrhotite and pyrite. SCOTT and BARNES (1971) carried out a work on the synthesis of sphalerite solid solution coexisting with pyrrhotite and pyrite in ammonium iodite and chloride aqueous solutions by the thermal gradient transporting method and made clear the phase relations of the sphalerite solid solution, troilite, pyrrhotite,

and pyrite in the system Fe–Zn–S and the relationship between the sphalerite composition, temperature, and sulfur fugacity. Godovikov and Ptitsin (1969) and Ptitsin and Godovikov (1971) synthesized the phases in the Cu_2S–Bi_2S_3 join by using the hydrothermal *in-situ* crystallizing method with an ammonium chloride solution at temperatures from 300° to 500°C, and from 250° to 300°C, respectively. Sugaki and Kitakaze (1972) synthesized alabandite solid solution associated with pyrrhotite and pyrite in an ammonium chloride solution and determined their phase relationship. Sugaki *et al.* (1975) succeeded in the hydrothermal synthesis of the three component phases of the Cu–Fe–S system, such as bornite, chalcopyrite, intermediate solid solution, and nukundamite etc. by the thermal gradient method, and obtained an isothermal phase diagram of the system. Sugaki *et al.* (1980) also synthesized wittichenite, emplectite, cuprobismutite, and phases $CuBi_3S_5$, and $Cu_8Bi_8S_{19}$, etc. belonging to the system Cu–Bi–S, by using the hydrothermal transporting method, and made clear the phase relations in the system. Recently, Sugaki *et al.* (1981b) studied on phase equilibrium in the quaternary system Cu–Fe–Bi–S in the same way and partly determined the complicated phase relations.

Although studies of the phase equilibrium of most of the sulfide system by the dry method, using an evacuated glass tube, have been carried out, as summarized by Barton and Skinner (1967) and Craig and Scott (1974), experimental works on hydrothermal synthesis and the phase relations of the sulfide system are not mentioned above. That is because only such systems as Fe–Zn–S, Fe–Mn–S, Cu–Fe–S, Cu–Bi–S, and Cu–Fe–Bi–S have been studied hydrothermally. However, hydrothermal synthesis is significant in getting near to natural conditions and has the advantage that its reaction is faster than the dry method and, as a result, equilibrium is obtained relatively easily. Accordingly, the phase relation at low temperatures, which cannot be solved by the dry method, may be made clear by this hydrothermal method. Thus, for example, from the polymetallic sulfide system studied under hydrothermal conditions, the phase relations in the Cu–Fe–Bi–S system are described in this paper. The sulfide phases in this study are shown in the Cu–Fe–Bi–S tetrahedron of Fig. 1. Their crystal data, such as chemical formula, crystal system, space group, and cell parameters are also given in Table 1.

2. *Experimental Procedures*

2.1 *Hydrothermal synthesis*

The thermal gradient transporting method is generally employed as a way of hydrothermally synthesizing sulfide minerals. In this method, sulfides as a nutrient are immediately dissolved at the hot end of a reaction tube, transported by convection across a small temperature gradient in an aqueous

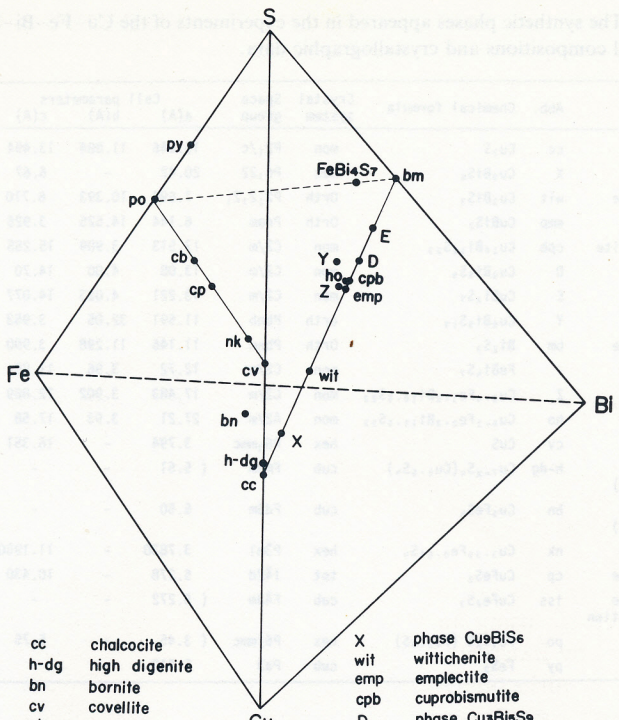

FIG. 1. Minerals and synthetic phases in the Cu–Fe–Bi–S system.

solution, and then reprecipitated as coexisting crystals at the cool end of the tube.

As a nutrient material, a mixture of powder sulfides was used which had been synthesized in advance by a reaction between pure metals (over 99.99% in purity) and 99.99% pure sulfur in an evacuated silica glass tube. Of the dry method using an evacuated glass tube, the papers of KULLERUD (1953, 1971), SUGAKI and SHIMA (1965a, b), and CRAIG and SCOTT (1974), furnish us with much information. Natural pure sulfides were sometimes used as a nutrient.

As a transporting solution, several kinds of aqueous solutions, such as potassium and sodium chloride or hydroxide, ammonium iodite and chloride, and lithium chloride were usually employed in varing concentrations. Among them, an ammonium chloride solution was the most adequate solvent, as reported by KUZ'MINA (1961), IKORNIKOVA (1962), CHERNYSHEV *et al.* (1968), SCOTT and BARNES (1971), and SUGAKI *et al.* (1975, 1976a). Most experiments

TABLE 1. The synthetic phases appeared in the experiments of the Cu–Fe–Bi–S system and their chemical compositions and crystallographic data.

Phases	Abb.	Chemical formula	Crystal system	Space group	Cell parameters a(A)	b(A)	c(A)	β
Chalcocite	cc	Cu_2S	mon	$P2_1/c$	15.246	11.884	13.494	116.35°
Phase X	X	Cu_9BiS_6	hex	$P6_322$	20.42	-	6.67	-
Wittichenite	wit	Cu_3BiS_3	Orth	$P2_12_12_1$	7.694	10.393	6.710	-
Emplectite	emp	$CuBiS_2$	Orth	Pnam	6.144	14.525	3.925	-
Cuprobismutite	cpb	$Cu_{10}Bi_{12}S_{23}$	mon	C2/m	17.513	3.909	15.255	101.09°
Phase D	D	$Cu_3Bi_5S_9$	mon	C2/m	13.08	4.00	14.70	99.4°
Phase E	E	$CuBi_3S_7$	mon	C2/m	13.221	4.023	14.077	115.46°
Phase Y	Y	$Cu_6Bi_6S_{19}$	orth	Pbnb	11.591	32.05	3.953	-
Bismuthinite	bm	Bi_2S_3	Orth	Pbnm	11.146	11.298	3.980	-
	-	$FeBi_4S_7$	mon	C2/m	12.72	3.96	11.80	104.5°
Phase Z	Z	$Cu_{8.4}Fe_{1.2}Bi_{10.8}S_{22}$	mon	C2/m	17.483	3.902	12.869	108.11°
Hodorushite	ho	$Cu_{8.1}Fe_{0.3}Bi_{11.5}S_{22}$	mon	A2/m	27.21	3.93	17.58	92.9°
Covellite	cv	CuS	hex	$P6_3mmc$	3.794	-	16.351	-
Digenite (high form)	h-dg	$Cu_{7-X}S_4(Cu_{6.6}S_4)$	cub	Fm3m	(5.51	-	-	-)
Bornite (high form)	bn	Cu_5FeS_4	cub	Fd3m	5.50	-	-	-)
Nukundamite	nk	$Cu_{3.39}Fe_{0.61}S_4$	hex	$P\bar{3}m1$	3.7830	-	11.1950	-
Chalcopyrite	cp	$CuFeS_2$	tet	$I\bar{4}2d$	5.278	-	10.430	-
Intermediate solid solution	iss	$CuFe_2S_3$	cub	$F\bar{4}3m$	(5.272	-	-	-)
Pyrrhotite	po	$Fe_{1-X}S$ ($Fe_{0.9}S$)	hex	P6/mmc	(3.45	-	5.75	-)
Pyrite	py	FeS_2	cub	Pa3	5.410	-	-	-)

on synthesis in the system Fe–Mn–S, Cu–Fe–S, and Cu–Fe–Bi–S by SUGAKI *et al.* (1972, 1975, 1981b) were thus performed using a 5 m ammonium chloride solution as the transporting solvent. SCOTT (1975) discussed the necessary factors for the aqueous solution as the recrystallizing agent, and mentioned that an ammonium halide solution is the most effective and stable solvent for metal sulfide transportation.

As a reaction vessel, a gold tube of 4 to 5 mm in inside diameter and about 50 mm in length was commonly used. The reaction tube must not react to either the transporting solution nor to the nutrient sulfides. Gold is stable enough in a 5 m ammonium chloride solution to 500°C, in 5 m ammonium iodite to 400°C, in 6 m sodium chloride to at least 500°C, in 4.5 m potassium chloride to at least 700°C, in 2 to 15 m sodium hydroxide to 700°C, and in 11.5 m potassium hydroxide solution to at least 500°C (SCOTT, 1974). Also, gold is not attacked in the general sulfide system, but it becomes unstable in the system containing large amounts of such metals as mercury, bismuth, and arsenic. In such cases, a sealed silica tube is used, but this permits only a limited range of temperatures, up to 500°C.

Several ten milligrams, 10 to 50 mg in common, of nutrient and 0.2 to 0.3 ml of solution were put into the gold tube and the tube was sealed by welding. The sealed gold tube was placed into a test tube-type pressure vessel

and heated in a vertical electric furnace designed so as to provide a linear thermal gradient by independently-controlled separate upper and lower heating elements. The temperature during the runs was measured by chromel-almel thermocouples inserted in two thermocouple walls at the top (or middle) and bottom portions of the outside wall of the pressure vessel. However, the inside temperature of the vessel was about 20° to 30°C lower than that of the outside at about 300°C. So the temperature crystallizing sulfide phases in the gold tube need to be directly measured in the pressure vessel. SUGAKI *et al.* (1980) measured temperature reprecipitated sulfide crystals by a thermocouple inserted into the inside of the vessel so as to get close to the top of the gold tube. When the thermal gradient is steep, the amount of sulfide crystallized was large, but metastable phases occurred. Therefore, a gentle thermal gradient was necessary in order to obtain an equilibrium condition, and the temperature difference between the top and bottom of the gold tube, 5 cm long, was kept between 5° to 20°C; that is, a thermal gradient of 1° to 4°C/cm. Pressure is measured by a Bourdon's tube gauge. At the termination of an experiment, the furnace was pulled down and the pressure vessel was cooled rapidly to room temperature in an air blast.

2.2 *Identification of phases*

Synthesized products were usually found in aggregate of several kinds of sulfides grown near the top of the gold tube. They were identified by means of a stereomicroscope, ore microscope, Gandolfi and Guinier cameras, and an electron probe microanalyser.

Because of the well-developed idiomorphic crystal forms, some synthesized phases could be quickly identified only by observation under a binocular microscope. Bornite commonly appeared as cubic, polyhedral crystals up to 300 μm in size, chalcopyrite as tetrahedral form, and pyrrhotite as hexagonal plates or prismatic crystals. Nukundamite occurred as beautiful, thin hexagonal platy forms up to 0.3 mm in diameter. However, it was difficult to distinguish intermediate solid solution from chalcopyrite by crystal form alone. Also, wittichenite appeared as rhombic, polyhedral forms of pale lead-gray in color, emplectite as thin platy or long prismatic crystals showing a lead-gray color, and phase $Cu_{8.4}Fe_{1.2}Bi_{10.8}S_{22}$ (Z) showed as short prismatic crystals of steel gray. Emplectite, cuprobismutite, phase $CuBi_3S_5$ (E), and phase $Cu_8Bi_8S_{19}$ (Y) were hard to distinguish from each other by their crystal shapes because they show forms similar to long prismatic or acicular forms. Metallic bismuth occurred as melted globules of about 200 μm in diameter. The scanning electron micrographs of the sulfide minerals crystallized in these synthetic experiments are shown in Figs. 2 and 3.

The ore microscope was very effective in identifying the mineral phases. A small amount of the product was mounted in a polyester resin, polished carefully, and observed under a reflecting microscope. Most hydrothermally

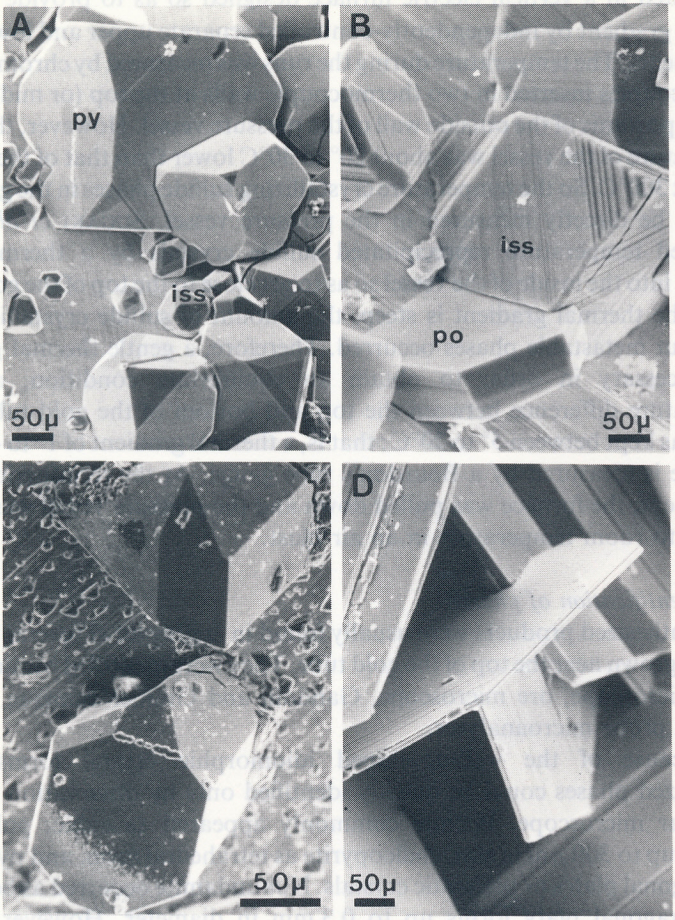

FIG. 2 A–D. Scanning electron micrographs of sulfide crystals synthesized hydrothermally. A, Pyrite and intermediate solid solution at 400°C; B, Pyrrhotite and intermediate solid solution at 300°C; C, Bornite at 420°C; D, Nukundamite at 420°C.

synthesized phases have optical properties similar to those of the equivalent natural minerals. The reflecting color of bornite solid solution varies from pinkish brown in copper-poor members to bluish gray in copper-rich ones, and also becomes a lighter brown with a bluish tint with increasing bismuth contents. Intermediate solid solution and chalcopyrite look very similar, but the former shows rather pinkish and less yellowish tints. Also, an iron-rich intermediate solid solution becomes lighter and less pinkish in color and is difficult to distinguish from chalcopyrite. Meanwhile, the copper-rich intermediate solid solution has usually fine lamellae of bornite or chalcopyrite

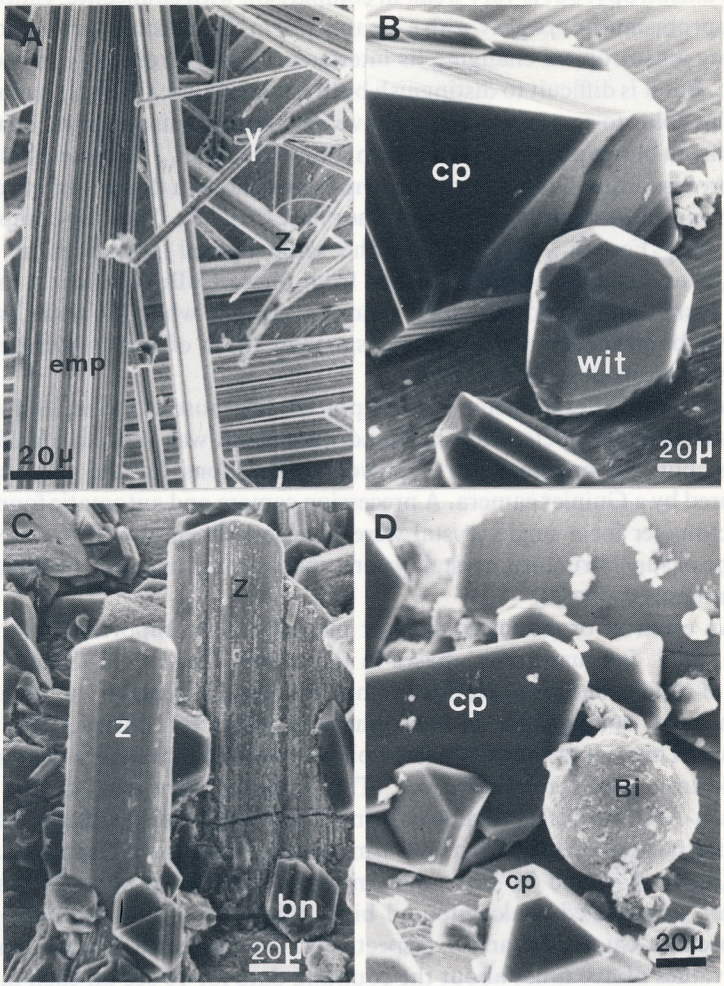

FIG. 3 A–D. Scanning electron micrographs of sulfide and sulfosalt crystals synthesized hydrothermally. A, Emplectite (tabular), phase Z (long prismatic) and phase Y (acicular) at 300°C; B, Wittichenite and chalcopyrite at 300°C; C, phase Z and bornite at 420°C; D, Chalcopyrite and bismuth liquid at 300°C.

as exsolution products segregated during cooling. Pyrrhotite is lighter and pinkish in color in comparison with iron-rich intermediate solid solution.

On the other hand, synthetic phases belonging to copper-bismuth sulfides have nearly the same optical properties, but some phases can be distinguished from others by their reflecting color and anisotropy. Wittichenite is darker gray color than emplectite, cuprobismutite, and phase $CuBi_3S_5$ (E). Also it

shows anisotropy, but is very weak in comparison with emplectite. Emplectite and cuprobismutite are gray with a creamy tint in the reflecting color and have a strong anisotropism changing its interference colors from gray to reddish-brown. But it is difficult to distinguish both phases. Phase $CuBi_3S_5$ has almost a similar color to emplectite, but it shows very strong anisotropism, changing colors from bluish purple to pale brown. Phase $Cu_8Bi_8S_{19}$ (Y) is nearly similar to cuprobismutite, but is slightly brownish and shows a distinct bireflectance and strong anisotropism, the same as the phase $CuBi_3S_5$. The four-component phase $Cu_{8.4}Fe_{1.2}Bi_{10.8}S_{22}$ (Z) has the same optical properties as phase $CuBi_3S_5$ and cannot be distinguished from phase $CuBi_3S_5$ under a microscope. Bismuthinite shows a light color of grayish white to white, with a stronger bireflectance and anisotropism than those of the copper-bismuth sulfide minerals described above.

An X-ray diffractometer was not practical because of the small quantity of synthesized products. Thus, a Gandorfi camera was used to identify the phases, but the precise data of powder diffractions for the phases were measured by a Guinier camera. A precession camera and automatic four circle diffractometer for a single crystal were occasionally employed to determine the type of superstructure, crystal system, space group, and cell constants, etc. for synthesized phases.

An electron probe microanalyser played a most important role in the phase study. Because many phases in the system Cu–Fe–Bi–S have some range of solid solutions at elevated temperatures, it is necessary to determine the chemical composition of each phase in order to construct the phase diagram. Thus, all of the synthesized phases were quantitatively analysed by the electron probe microanalyser. The analyses were carried out by a Shimazu-ARL EMX-II instrument using 20 kV accelerating voltage, 0.02 μA specimen current on chalcopyrite, 3 μm spot size, and curved crystals LiF for Cu–Kα, Fe–Kα, and Bi–Lα radiations, and ADP for S–Kα. As standard samples, synthesized chalcocite and bismuthinite, and natural chalcopyrite were used for Cu, Bi, Fe, and S, respectively. The measured X-ray intensities, mean values of five times about the counting data for 10 sec on each mineral grain and standard, were corrected for background and dead time effects. Chemical compositions were calculated by the BENCE and ALBEE (1968) procedure using the alfa-factor for the Cu–Fe–Bi sulfide system (SUGAKI *et al.*, 1974, 1976b). Mineral grains having exsolved phases were first heated in an evacuated glass tube at the same temperature as those synthesized, and then quenched in ice water. In some specimens, such as intermediate solid solution and bornite solid solution, complete homogenization was not achieved in this way, but even so, the exsolution texture became sufficiently fine to allow analysis of the bulk composition of the phase by an electron probe microanalyser.

3. *Experimental Results and Phase Relation*

3.1 *The system Cu–Fe–S*

Minerals which belong to the system Cu–Fe–S are the most important among ore minerals because they are persistent minerals occurring in many kinds of ore deposits. Accordingly, phase relations in the Cu–Fe–S system are of great geological interest, and have been studied for more than 30 years since the first study was made by MERWIN and LOMBARD (1937) by such authors as SCHLEGEL and SCHÜLLER (1952), ROSEBOOM and KULLERUD (1958), BRETT (1963), YUND and KULLERUD (1966), KULLERUD *et al.* (1969), MUKAIYAMA and IZAWA (1970), CABRI (1973), and BARTON (1973). They carried out a large number of systematic experiments on this system and determined the phase relations to be between 700° and 200°C. Bornite, pyrrhotite, and intermediate solid solutions occur in the system at high temperatures. The latter forms an extensive field in the central portion of the system. These solid solutions associate with pyrite and chalcopyrite. However, as the temperature falls, various phase-changing reactions take place and the phase relations become very complicated, but have not been elucidated in detail. Especially after the new phases, talnakhite, mooihoekite, and haycockite, had been found by CABRI and his co-workers (1967, 1971, 1972), the phase relations at low temperatures were seen to be much more complicated. Many problems remain unsolved. There is also the problem of sluggish reaction rates at low temperatures in addition to the complexity of the phase relations in the system. All the experiments done by the authors mentioned above were performed by the dry method using the evacuated silica glass tube. SUGAKI *et al.* (1975) tried hydrothermal synthesis of copper and iron sulfides using the thermal gradient method and obtained isothermal phase diagrams of the system Cu–Fe–S at 300° and 350°C.

3.1.1 *The isothermal section at 400°C*

In order to determine the 400°C isothermal phase relation of the Cu–Fe–S system as a continuous work of SUGAKI *et al.* (1975), hydrothermal experiments were performed by the present authors. Crystallized mineral phases were determined from crystal shapes, optical properties, and X-ray powder data etc., and microprobe analyses were performed on each of the phases synthesized. Figure 4 is a part of the phase diagram of the system Cu–Fe–S at 400°C obtained from the experimental data. Seven stable phases are shown, but do not include the three end member elements. They are bornite solid solution, chalcopyrite solid solution, intermediate solid solution, pyrrhotite solid solution, covellite, nukundamite, and pyrite. Among them, the intermediate and bornite solid solutions have extensive composition fields, while chalcopyrite and pyrrhotite solid solutions have limited ones. The following ten univariant phase assemblages are as stable at 400°C as those at 350°C in the experiments carried out by SUGAKI *et al.* (1975): covellite +

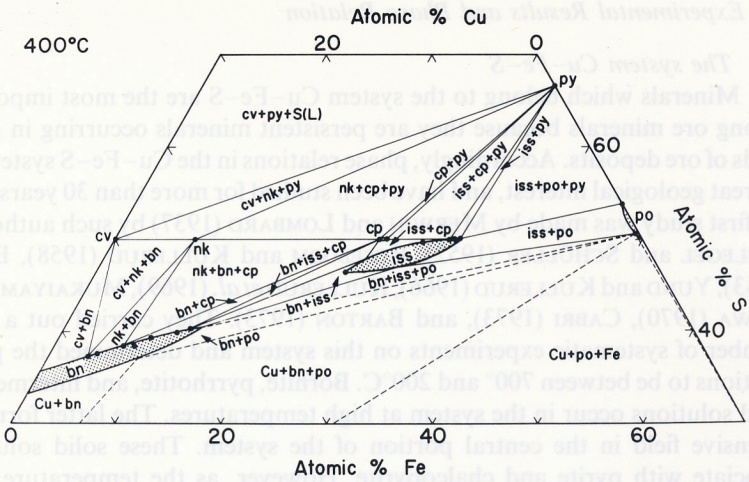

FIG. 4. Phase relations in the central portion of the Cu–Fe–S system at 400°C under hydrothermal conditions. Solid circles show the analytical compositions of the synthetic phases. Abbreviations in this figure are shown in Table 1 and Fig. 1.

pyrite + sulfur (L), covellite + nukundamite + pyrite, nukundamite + chalcopyrite + pyrite, intermediate solid solution + chalcopyrite + pyrite, intermediate solid solution + pyrrhotite + pyrite, covellite + bornite solid solution + nukundamite, bornite solid solution + nukundamite + chalcopyrite, bornite solid solution + chalcopyrite + intermediate solid solution, bornite solid solution + intermediate solid solution + pyrrhotite, bornite solid solution + pyrrhotite + copper. The last two assemblages, which have low sulfur fugacities, have not been observed in the present study.

The chalcopyrite solid solution field at 400°C is not so wide as YUND and KULLERUD (1966) and BARTON and SKINNER (1967) have suggested, and has a limited range from nearly stoichiometric $CuFeS_2$ to $Cu_{0.98}Fe_{1.02}S_{2.00}$. The range corresponds to 1.00 to 0.96 in the Cu/Fe atomic ratio along a line of metal to a sulfur ratio of approximately 1.0. Compositions of chalcopyrite coexisting with bornite and/or nukundamite concentrate into stoichiometric $CuFeS_2$ and the chalcopyrite in the univariant assemblage with the intermediate solid solution and pyrite becomes most iron-rich. The intermediate solid solution, as stated above, has a considerably wide field extending from near the stoichiometric cubanite composition toward the copper-rich and sulfur-deficient mooihoekite composition at 400°C, as is clearly seen in Fig. 4. The field includes the high temperature cubic phase of cubanite as well as the composition of mooihoekite and haycockite described by CABRI and HALL (1972). Although the iron-rich and copper-rich ends of the solid solution field have not been determined precisely, the most copper-rich phase of the intermediate solid solution synthesized at 400°C was the

composition of Cu 40.5, Fe 27.9, and S 31.7 in a weight percent which gives the formula of $Cu_{1.80}Fe_{1.41}S_{2.79}$ with Cu/Fe atomic ratio of 1.28. The intermediate solid solution coexists stably with pyrite, pyrrhotite, chalcopyrite, and bornite solid solution. The composition of the intermediate solid solution in equilibrium with pyrite and pyrrhotite is Cu 24.1, Fe 40.1, and S 35.2 in a weight percent corresponding to $Cu_{1.04}Fe_{1.96}S_{3.00}$, which is very close to stoichiometric cubanite ($CuFe_2S_3$). Also, the composition of the intermediate solid solution in the univariant assemblage with chalcopyrite and pyrite is Cu 25.5, Fe 38.2, and S 34.7 in weight percent ($Cu_{1.11}Fe_{1.90}S_{3.00}$).

The boundary of the sulfur-rich part of the bornite solid solution field at 400°C was determined by means of microprobe analysis on the bornite coexisting with other sulfide phases. The boundary coincides approximately with the $Cu_{1.8}S$–Cu_5FeS_4 join, but there are no data for the metal-rich parts of the composition field because synthesis of the bornite solid solution with low sulfur fugacity assemblages is difficult. The bornite solid solution field extends far beyond its stoichiometric composition toward a more iron-rich side. The maximum iron content of the solid solution was 13.4 in weight percent (3.97 in Cu/Fe atomic ratio, $Cu_{4.76}Fe_{1.20}S_{4.04}$). The bornite solid solution associates with covellite, nukundamite, chalcopyrite, intermediate solid solution (and pyrrhotite). Bornite with a composition of more than 13.4 weight percent iron (less than 3.97 in the Cu/Fe atomic ratio) was in an equilibrium with only the intermediate solid solution. Also, bornite assembled with only chalcopyrite has a considerable composition range from 13.4 ($Cu_{4.76}Fe_{1.20}S_{4.04}$) to 7.1 ($Cu_{5.52}Fe_{0.65}S_{3.83}$) in weight percent of iron (3.97 to 8.49 in Cu/Fe atomic ratio), which includes the stoichiometric composition of bornite. The composition of bornite in the univariant assemblage of bornite, chalcopyrite, and intermediate solid solution is Cu 60.7, Fe 13.4, and S 26.0 in weight percent ($Cu_{4.76}Fe_{1.20}S_{4.04}$). Bornite associated with chalcopyrite and nukundamite has a composition of Cu 68.5, Fe 7.1, and S 24.0 in weight percent (8.49 in Cu/Fe atomic ratio, $Cu_{5.52}Fe_{0.65}S_{3.83}$). The bornite composition in equilibrium with covellite and nukundamite was given as Cu 72.2, Fe 3.4, and S 22.9 in weight percent (18.6 in the Cu/Fe atomic ratio, $Cu_{5.95}Fe_{0.32}S_{3.73}$) nearly close to the digenite composition.

Nukundamite always occurs in a crystal of thin hexagonal plates, as shown in Fig. 2-D. The chemical composition of nukundamite synthesized at 400°C is Cu 56.5, Fe 9.4, and S 34.0 in weight percent and is almost equivalent to $Cu_{3.38}Fe_{0.62}S_{4.00}$ ($Cu_{5.5}FeS_{6.5}$). These values are in good accordance with those of idaite (nukundamite) produced by the dry method using the evacuated glass tube (YUND, 1963) and synthesized hydrothermally at 350°C by SUGAKI *et al.* (1975). The crystal structure data of nukundamite synthesized hydrothermally were also given by SUGAKI *et al.* (1981a). Nukundamite can coexist stably with pyrite, covellite, bornite, and chalcopyrite. Because the tie line between nukundamite and chalcopyrite occurs in a stable assemblage at

400°C, the same as the isothermal section at 350° and 300°C reported by SUGAKI *et al.* (1975), the assemblage of bornite and pyrite previously accepted by YUND and KULLERUD (1966), was not found in this study.

3.1.2 The 300°C isothermal section

In order to construct an isothermal phase diagram of the system Cu–Fe–S at 300°C, hydrothermal experimental runs were carried out by SUGAKI *et al.* (1975). The work has been continued by the present authors using the same method because the experimental runs were insufficient. The phase diagram in the central portion of the system Cu–Fe–S, which is the result of data compiled from both experiments, is shown in Fig. 5. Except for a small reduction of the solid solution fields and the tie line change from the intermediate solid solution-pyrite join to the chalcopyrite-pyrrhotite join, the phase relations of the system are essentially the same as those at 400°C, as mentioned above. The stable phases in the system at 300°C are chalcopyrite, bornite solid solution, intermediate solid solution, pyrrhotite, nukundamite, covellite, and pyrite excluding digenite (high form) solid solution and end-member elements.

Solid solution ranges of chalcopyrite at 300°C are about the same or slightly increased in comparison with those at 400°C. The most iron-rich chalcopyrite, which coexists with pyrrhotite and intermediate solid solution, has a composition of $Cu_{0.97}Fe_{1.04}S_{1.99}$. The chalcopyrite solid solution extends from 1.0 to approximately 0.93 in the Cu/Fe atomic ratio along the line of the metal/sulfur atomic ratio 1.0. The intermediate solid solution, still having a remarkable area in the system at 300°C, extends between the Cu/Fe

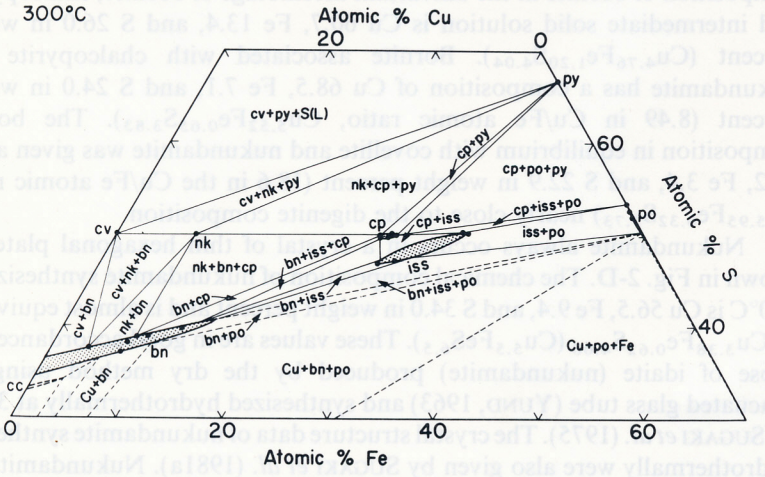

FIG. 5. Phase relations in the central portion of the Cu–Fe–S system at 300°C under hydrothermal conditions.

atomic ratio of 0.51 and 1.04, and has a composition of $Cu_{1.01}Fe_{1.97}S_{3.02}$ in equilibrium with hexagonal pyrrhotite and chalcopyrite, while the phase $Cu_{1.63}Fe_{1.57}S_{2.81}$ coexists with bornite and chalcopyrite. The solid solution field includes the compositions of mooihoekite $Cu_9Fe_9S_{16}$ and haycockite $Cu_4Fe_5S_8$. The composition of the intermediate solid solution, coexisting with chalcopyrite and pyrrhotite, is Cu 23.5, Fe 40.1, and S 35.4 in weight percent (Cu/Fe atomic ratio of 0.51, $Cu_{1.01}Fe_{1.97}S_{3.02}$), which is very close to stoichiometric cubanite $CuFe_2S_3$. The tie line between the intermediate solid solution and pyrite, existing stably at 350° and 400°C, is replaced by the tie line between chalcopyrite and pyrrhotite at 300°C. The tie line change was determined at 328° ± 5°C by YUND and KULLERUD (1966). Also, SUGAKI *et al.* (1982) recently found that the tie line was not changed at 330°C but changed to the chalcopyrite-pyrrhotite join at 320°C under hydrothermal conditions at pressures of 1,000 to 2,000 kg/cm^2.

Although the bornite solid solution becomes less extensive at 300°C than at 400°C, the field extends still far beyond the stoichiometric composition of bornite toward the iron-rich composition. The maximum iron content of the bornite solid solution is approximated by the composition of bornite coexisting with intermediate solid solution, that is, Cu 57.2, Fe 15.7, and S 26.2 in weight percent (Cu/Fe atomic ratio of 3.19, $Cu_{4.50}Fe_{1.41}S_{4.09}$). Meanwhile, bornite in equilibrium with chalcopyrite has a wide compositional range from about 3.5 to 7.2 in the Cu/Fe atomic ratio at 300°C. The composition of bornite coexisting with chalcopyrite and nukundamite is Cu 69.2, Fe 7.6, and S 24.3 in weight percent (Cu/Fe atomic ratio of 7.96, $Cu_{5.49}Fe_{0.69}S_{3.82}$). Nukundamite occurs in equilibrium associations with covellite, bornite, chalcopyrite, and pyrite. The assemblage of nukundamite and chalcopyrite is also stable at 300°C, the same as at 350° and 400°C. The mean values of the microprobe analysis for nukundamite synthesized at 300°C are Cu 57.1 ± 0.2, Fe 9.0 ± 0.4, and S 33.9 ± 0.2 in weight percent (Cu/Fe atomic ratio of 5.5 ± 0.2, a metal sulfur ratio of approximately 1.0). Nukundamite has no field of solid solution at 300°C, and its composition is very close to $Cu_{3.38}Fe_{0.62}S_{4.00}$ or $Cu_{5.5}FeS_{6.5}$, as proposed by SUGAKI *et al.* (1981a), YUND (1963), and YUND and KULLERUD (1966). All pyrrhotite synthesized at 300°C were found to be of a hexagonal type as a result of reexamination by this study and SUGAKI *et al.* (1977), although SUGAKI *et al.* (1975) reported that pyrrhotite has two structure types at 300°C, hexagonal and monoclinic. Pyrrhotite assembles with pyrite, chalcopyrite, intermediate solid solution, and bornite solid solution. But, the last assemblage could not be seen in these experimental runs.

3.2 The system Cu–Bi–S

In the system Cu–Bi–S, several common copper bismuth sulfosalt minerals, such as wittichenite, emplectite, and cuprobismutite, etc. were

known widely. Synthetic experiments on these minerals have been carried out by several authors (GAUDIN and DICKE, 1939; NUFFIELD, 1947, 1952; GODOVIKOV and PTITSIN, 1969; CHEN and CHANG, 1974). However, the phase equilibrium of the system has not been performed by so many authors. The binary Cu_2S–Bi_2S_3 join was studied by BUHLMANN (1971), SUGAKI and SHIMA (1972), FEDOROVA (1972), and SUGAKI *et al.* (1980), and the ternary Cu–Bi–S system was investigated by SUGAKI and SHIMA (1971). However, these studies were performed almost exclusively by the dry method using an evacuated glass tube. One exception is the work by SUGAKI *et al.* (1980) who employed the hydrothermal transport method for the synthesis of copper bismuth sulfosalts. The results of the experiments on phase relations in the binary Cu_2S–Bi_2S_3 and the ternary Cu–Bi–S system are mentioned below.

3.2.1 The binary Cu_2S–Bi_2S_3

The phase diagram of the binary Cu_2S–Bi_2S_3 experimental data, summarized by SUGAKI and SHIMA (1972) and SUGAKI *et al.* (1980), is shown in Fig. 6. As the crystalline phases, chalcocite (Cu_2S), phase Cu_9BiS_6 (X), wittichenite (Cu_3BiS_3), emplectite ($CuBiS_2$), cuprobismutite ($Cu_{10}Bi_{12}S_{23}$), phase $Cu_3Bi_5S_9$ (D), phase $CuBi_3S_5$ (E), and bismuthinite (Bi_2S_3) are found in the binary of Fig. 6. The phases Cu_9BiS_6, $Cu_3Bi_5S_9$, and $CuBi_3S_5$ have not been found in nature. Phase $CuBi_3S_5$ is stable below 649 ± 5°C and incongruently melts at this temperature to Bi_2S_3 and liquid. The phase $Cu_3Bi_5S_9$ is stable in the temperature range between $442° \pm 5$°C and $620° \pm 5$°C, at which it incongruently melts to phase $CuBi_3S_5$ and liquid. It dissolves a considerable amount of the Cu_2S molecule in solid solution, and its maximum limit is 56.5 mole percent Bi_2S_3 at 523°C. Synthetic wittichenite is identical with the natural one in every respect. Though it has the composition of stoichiometric Cu_3BiS_3 at room temperature, it forms a solid solution in a

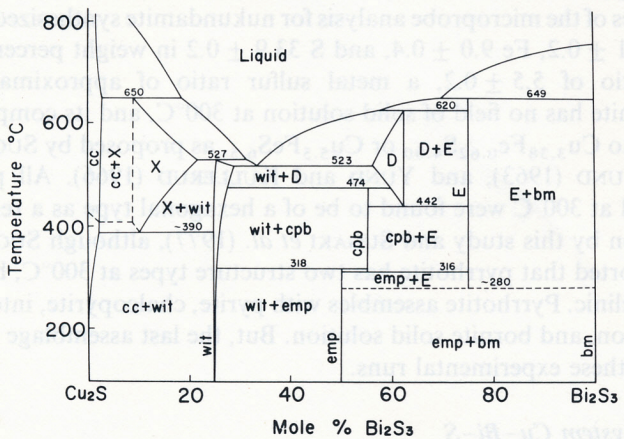

FIG. 6. Phase diagram of the Cu_2S–Bi_2S_3 system after SUGAKI and SHIMA (1972) and SUGAKI *et al.* (1980).

very limited range, shifting toward Cu_2S poor composition at high temperature (Fig. 6). The solid solution of wittichenite extends from 26.5 to 28.5 mole percent Bi_2S_3 at 500°C. The solid solution of nearly 27.5 mole percent Bi_2S_3 incongruently melts at 527 ± 5°C. The eutectic point between wittichenite solid solution and the solid solution of phase $CuBi_3S_5$ is 527 ± 5°C at about 35 mole percent Bi_2S_3. The phase Cu_9BiS_6 is stable between about 650° and 390°C, but a lower stability limit has not been determined. It dissolves a considerable amount of Bi_2S_3 molecules and the solid solution field extends to 13 mole percent Bi_2S_3 at 450°C, 22 mole percent Bi_2S_3 in maximum at 527°C. The phase relation between emplectite and cuprobismutite was one of the important problems in this join. Cuprobismutite, found by Hillebrand in 1884, was first given a chemical composition of 3 $(Cu, Ag)_2S \cdot 4Bi_2S_3$. DANA (1892) and SCHNEIDERHÖHN and RAMDOHR (1931) described this mineral, but SHORT (1931) and PALACHE (1940) denied its existence. However, NUFFIELD (1952), by re-examination on the type specimens from the Missouri mine, identified cuprobismutite as a varied species with a chemical composition of $CuBiS_2$ and suggested a dimorphous relationship with emplectite. BUHLMANN (1971) stated that the low temperature polymorph of emplectite (β-$CuBiS_2$) inverts to the high form of cuprobismutite (α-$CuBiS_2$) at 290°C, while SUGAKI and SHIMA (1972) reported that the composition of cuprobismutite is not $CuBiS_2$ but $Cu_{24}Bi_{26}S_{51}$ and the inversion temperature between both phases might be about 360°C from the DTA experiment. In order to make more clear the phase relation between them, SUGAKI *et al.* (1980) have carried out detailed experiments under the dry and hydrothermal conditions. Figure 7 shows a central portion of the binary Cu_2S–Bi_2S_3 at a low temperature obtained by both the dry and hydrothermal methods, and compiled from the experimental data of SUGAKI *et al.* (1980) and from recent work by the present authors. From the results of these experiments, emplectite and cuprobismutite are not in dimorph, but are two independent minerals with different compositions. Emplectite has a stoichiometric composition of $CuBiS_2$, but cuprobismutite has a little bismuth-rich composition of $Cu_9Bi_{11}S_{21}$, described by TAYLOR *et al.* (1973), as being $Cu_{10}Bi_{12}S_{23}$, as is the composition of natural cuprobismutite. Emplectite is only stable below 318° ± 3°C, while cuprobismutite is never synthesized below 316° ± 3°C. There is a narrow field of coexistence of both minerals at temperatures from 316° to 318°C in a composition range from 50 to 54.5 mole percent Bi_2S_3. The phase $CuBi_3S_5$ is stable above approximately 280°C and does not appear below this temperature, but the assemblage of emplectite and bismuthinite forms as those found in natural ores. Thus, the phase $CuBi_3S_5$ could not be expected to be found in nature, though SUGAKI and SHIMA (1972) mentioned that it could possibility be found so in the future, while wittichenite could not associate with bismuthinite in an equilibrium state. During all the experiments on the

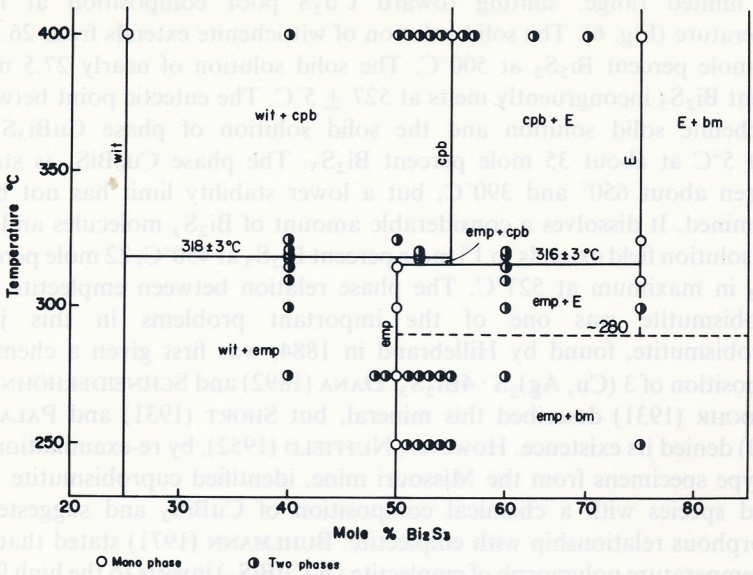

FIG. 7. The phase relations of a central part in the join Cu_2S–Bi_2S_3 of Fig. 6.

synthesis and phase equilibrium of the binary Cu_2S–Bi_2S_3, klaprothite and dognacskite have not appeared. Both minerals, having $Cu_6Bi_4S_9$ and $Cu_2Bi_4S_7$ in composition, could not be expected to be found hereafter.

3.2.1 The ternary Cu–Bi–S

The phase relations of the ternary system Cu–Bi–S at 300°, 400°, and 500°C were determined by using the method of the evacuated glass tube (SUGAKI and SHIMA, 1971). The isothermal section of the phase diagram in the system at 300°C is shown in Fig. 8. In this figure, high digenite solid solution, covellite, wittichenite, emplectite, phase $CuBi_3S_5$ (E), bismuthinite, and phase $Cu_8Bi_8S_{19}$ (Y) are shown as stably crystalline phases, and 12 univariant assemblages are found as follows: sulfur (L) + covellite + phase $Cu_8Bi_8S_{19}$, sulfur (L) + phase $Cu_8Bi_8S_{19}$ + bismuthinite, phase $Cu_8Bi_8S_{19}$ + bismuthinite + phase $CuBi_3S_5$, phase $Cu_8Bi_8S_{19}$ + phase $CuBi_3S_5$ + emplectite, phase $Cu_8Bi_8S_{19}$ + emplectite + wittichenite, covellite + phase $Cu_8Bi_8S_{19}$ + wittichenite, high digenite + covellite + wittichenite, bismuthinite + phase $CuBi_3S_5$ + bismuth (L), phase $CuBi_3S_5$ + emplectite + bismuth (L), wittichenite + emplectite + bismuth (L), wittichenite + high digenite + bismuth (L), and high digenite + copper + bismuth (L). The phase $Cu_8Bi_8S_{19}$, which was found by SUGAKI and SHIMA (1971), GODOVIKOV *et al.* (1971), and SUGAKI *et al.* (1972a), assembles with many phases, such as covellite, wittichenite, emplectite, phase $CuBi_3S_5$, bismuthinite, and sulfur at 300°C, but cannot coexist with high digenite, copper, and bismuth. Bismuthinite, em-

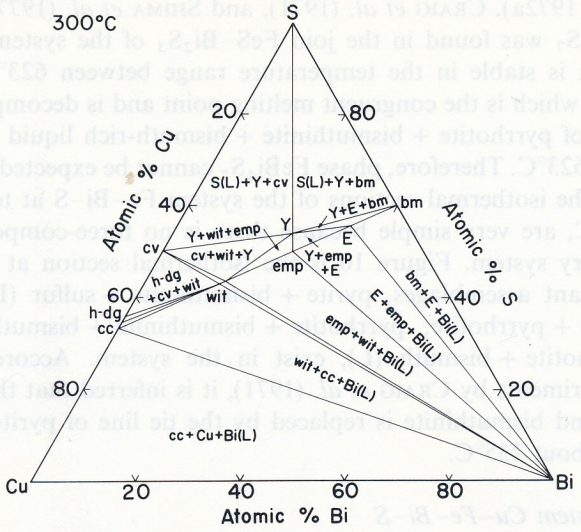

FIG. 8. Phase relations of the Cu–Bi–S system at 300°C obtained under dry conditions by SUGAKI and SHIMA (1971).

plectite, wittichenite, and high digenite can coexist with bismuth at 300°C, as is commonly seen in bismuth bearing ores.

At 400°C, emplectite does not form, but cuprobismutite appears. The phase relations in the isothermal section at 400°C are similar to those at 300°C, being exclusive of the appearance of phase Cu_9BiS_6 and cuprobismutite. There are 15 univariant assemblages. These are as follows: phase $Cu_8Bi_8S_{19}$ + bismuthinite + sulfur (L), phase $Cu_8Bi_8S_{19}$ + covellite + sulfur (L), phase $Cu_8Bi_8S_{19}$ + phase $CuBi_3S_5$ + bismuthinite, phase $Cu_8Bi_8S_{19}$ + cuprobismutite + phase $CuBi_3S_5$, wittichenite + phase $Cu_8Bi_8S_{19}$ + cuprobismutite, covellite + wittichenite + phase $Cu_8Bi_8S_{19}$, covellite + phase Cu_9BiS_6 + wittichenite, covellite + high digenite + phase Cu_9BiS_6, (chalcocite + high digenite + phase Cu_9BiS_6), bismuthinite + phase $CuBi_3S_5$ + bismuth (L), phase $CuBi_3S_5$ + cuprobismutite + bismuth (L), cuprobismutite + wittichenite + bismuth (L), wittichenite + phase Cu_9BiS_6 + bismuth (L), phase Cu_9BiS_6 + chalcocite + bismuth (L), and chalcocite + copper + bismuth (L).

Wittichenite, cuprobismutite and phase Cu_9BiS_6 form a very limited range of the solid solution at 400°C, while phases $Cu_8Bi_8S_{19}$ and $CuBi_3S_5$ have a stoichiometric composition at this temperature. Bismuth liquid dissolves some of the copper and sulfur.

3.3 The system Fe–Bi–S

Phase relations in the Fe–Bi–S system have been investigated by SUGAKI

et al. (1970, 1972a), Craig *et al.* (1971), and Shima *et al.* (1977). Synthetic phase $FeBi_4S_7$ was found in the join $FeS-Bi_2S_3$ of the system, as shown in Fig. 9. It is stable in the temperature range between 623° ± 3°C and 726° ± 3°C, which is the congruent melting point and is decomposed to the assemblage of pyrrhotite + bismuthinite + bismuth-rich liquid at temperatures below 623°C. Therefore, phase $FeBi_4S_7$ cannot be expected to be found in nature. The isothermal sections of the system Fe–Bi–S at temperatures below 623°C, are very simple because there is no three-component phase in the ternary system. Figure 10 is the isothermal section at 300°C, and four univariant assemblages, pyrite + bismuthinite + sulfur (L), pyrite + bismuthinite + pyrrhotite, pyrrhotite + bismuthinite + bismuth (L), and iron + pyrrhotite + bismuth (L), exist in the system. According to the data of experiments by Craig *et al.* (1971), it is inferred that the tie line of pyrrhotite and bismuthinite is replaced by the tie line of pyrite and bismuth below about 235°C.

3.4 The system Cu–Fe–Bi–S

In order to determine the isothermal phase relation in the quaternary system Cu–Fe–Bi–S, the experiments of hydrothermal syntheses, as mentioned above, were carried out by Sugaki *et al.* (1981b) at 420° and 300°C. The phases that appeared in the experiment were bornite, chalcopyrite, intermediate solid solution, pyrrhotite, and nukundamite belonging to the ternary Cu–Fe–S, phase Cu_9BiS_6, wittichenite, emplectite, cuprobismutite, phase $CuBi_3S_5$, phase $Cu_8Bi_8S_{19}$, bismuthinite and bismuth liquid in the ternary Cu–Bi–S, and phase $Cu_{8.4}Fe_{1.2}Bi_{10.8}S_{22}$ (Z) in the quaternary Cu–Fe–Bi–S system. Phases $Cu_3Bi_5S_9$ (D) and $FeBi_4S_7$ did not appear

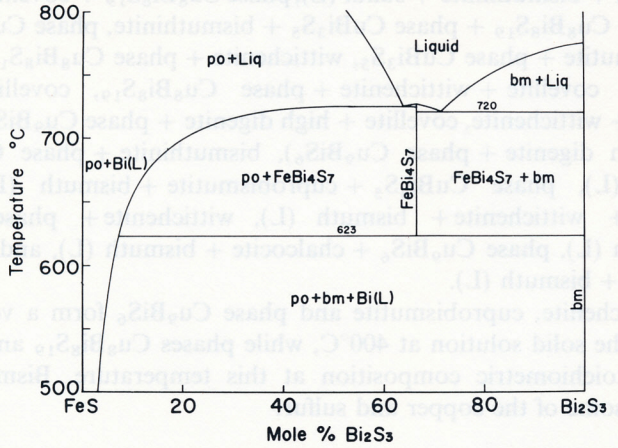

Fig. 9. Phase diagram of pseudo-binary system $FeS-Bi_2S_3$ under dry conditions after Shima *et al.* (1977).

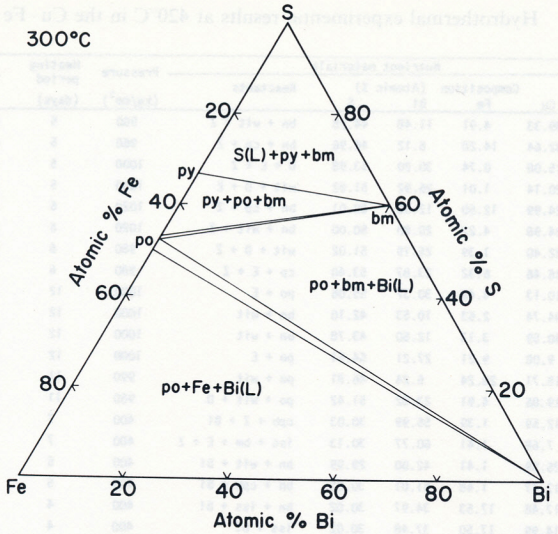

FIG. 10. Phase relations of the Fe–Bi–S system under dry conditions obtained by SUGAKI *et al.* (1970).

because they are unstable at 420°C or below. The experiments of SUGAKI *et al.* (1981b) were mainly performed under comparatively high sulfur fugacity because most of the bulk composition of nutrient materials were sulfur-rich and iron-poor. Thus, the appearance of bismuth and pyrrhotite was rare. The present study continues the work of SUGAKI *et al.* (1981b) and focusses on the phase relation of comparatively low sulfur fugacity to obtain the tie line with bismuth (liquid). A gold tube was generally used as a sample container in this experiment, but a silica tube had to be employed in the case of the experiments containing a fair amount of bismuth metals, because bismuth reacts on the gold tube. In this paper, the phase relations obtained by both experimental runs are described together.

3.4.1 The phase relations at 420°C

The results of the experimental runs at 420°C, together with the bulk composition and the phase assemblages of nutrient materials, the experimental conditions, and the synthesized phase assemblages, are given in Table 2. Synthesized products were usually composed of three or four solid phases, and occasionally of two phases, which seemed to be in equilibrium with each other. The phase assemblages at 420°C, seen in the table, were controlled principally by a composition of nutrient and sulfur fugacity within the gold or silica tubes. Sulfur fugacity was directly fixed by the bulk composition of nutrients. The principle mineral phases in the system, such as bornite, chalcopyrite, intermediate solid solution, pyrrhotite, nukundamite, wittichenite, cuprobismutite, phases Cu_9BiS_6, $CuBi_3S_5$, $Cu_8Bi_8S_{19}$, and

TABLE 2. Hydrothermal experimental results at 420°C in the Cu–Fe–Bi–S system.

Run No.	Nutrient materials Composition (Atomic %) Cu	Fe	Bi	S	Reactants	Pressure (kg/cm^2)	Heating period (days)	Synthesized phases
HCFB 027	39.33	4.91	11.48	44.28	bn + wit + Z	960	5	bn + cpb
HCFB 028	32.64	14.28	6.12	46.96	bn + cp + Z	960	5	bn + cp + Z
HCFB 031	15.08	0.74	30.20	53.98	D + E + Z	1000	5	cpb + E + Z
HCFB 032	20.14	1.01	26.92	51.92	wit + D + E	1000	5	cpb + E
HCFB 037	24.99	12.50	12.50	50.01	bn + cp + Z	1020	6	cpb + E + Z
HCFB 038	24.98	4.22	20.80	50.00	bn + wit + Z	1020	6	bn + cpb + Z
HCFB 043	22.40	1.39	25.19	51.02	wit + D + Z	980	6	bn + cpb
HCFB 044	16.46	6.32	23.87	53.40	cp + E + Z	980	6	bn + cp + nk + Z
HCFB 045	10.13	4.45	30.37	55.06	po + E	1000	12	cp + bm + E + Y
HCFB 046	44.74	2.63	10.53	42.10	bn + wit	1000	12	bn + wit
HCFB 047	40.59	3.13	12.50	43.78	bn + wit	1000	12	bn + wit + cpb
HCFB 048	9.08	9.21	27.21	54.51	po + E	1000	12	cp + E + Z
HCFB 052	18.71	28.24	6.24	46.81	po + wit	990	11	cp + E
HCFB 053	19.86	4.91	23.82	51.42	po + wit + D	960	11	bn + Z
HCFB 077*	12.59	1.39	55.99	30.03	cpb + Z + Bi	400	7	wit + cpb + Bi
HCFB 078*	7.68	1.41	60.77	30.13	iss + bm + E + Z	400	7	E
HCFB 079*	26.59	1.41	42.00	29.99	bn + wit + Bi	400	5	wit + Bi
HCFB 080*	17.47	1.48	51.01	30.05	bn + cpb + Bi	400	5	wit + Bi
HCFB 089*	17.48	17.53	34.97	30.02	bn + iss + Bi	400	4	bn + Bi
HCFB 090*	14.99	17.50	37.48	30.02	iss + Bi	400	4	bn + iss + Bi
HCFB 091*	15.99	14.98	38.99	30.04	bn + iss + Bi	400	4	bn + Z + Bi
HCFB 092*	12.49	17.52	39.97	30.02	iss + Bi	400	4	iss + po + Bi
HCFB 093*	24.07	7.01	38.48	30.07	bn + Z + Bi	400	11	bn + wit + Bi
HCFB 094*	21.00	6.98	42.00	30.02	bn + Z + Bi	400	11	bn + wit + Bi
HCFB 095*	20.99	10.52	38.49	30.00	bn + iss + Z + Bi	400	11	bn + Bi
HCFB 096*	17.48	10.54	41.98	30.01	bn + iss + Z + Bi	400	11	bn + wit + Bi
HCFB 107*	5.00	22.48	42.48	30.04	iss + po + bm + Bi	400	8	iss + po + Bi
HCFB 108*	33.57	1.39	34.96	30.08	bn + wit + Bi	400	13	wit + X + Bi
HCFB 109*	6.99	7.00	55.95	30.06	iss + Z + Bi	400	13	po + E + Bi
HCFB 110*	22.47	14.02	33.47	30.04	bn + iss + Bi	400	13	bn + Bi
HCFB 123*	10.50	10.51	49.00	29.99	iss + bm + E + Bi	400	9	bn + Z + Bi
HCFB 124*	14.00	7.02	49.00	29.99	bn + iss + Z + Bi	400	9	wit + Bi
HCFB 125*	30.09	1.34	38.49	30.09	bn + wit + cpb + Bi	400	9	wit + X + Bi
HCFB 126*	44.96	1.40	23.60	30.04	bn + X + Bi	400	9	wit + X + Bi
HCFB 127*	10.00	22.50	37.51	29.99	iss + po + Bi	400	9	iss + po + Bi
HCFB 128*	16.90	13.54	40.57	28.97	bn + iss + Z + Bi	400	9	bn + Z + Bi
HCFB 130*	10.14	13.51	47.32	29.03	iss + Z + Bi	400	7	bn + Z + Bi
HCFB 131*	6.76	13.52	50.69	29.03	iss + bm + Bi	400	7	iss + po + Bi
HCFB 132*	10.49	1.41	58.05	30.05	cpb + Z + Bi	400	6	cpb + E + Bi
HCFB 133*	19.99	14.01	35.98	30.02	bn + iss + Bi	400	6	bn + Z + Bi
HCBS 043	19.05	0.00	28.57	52.38	cpb + E	350	5	cpb + wit + Y
HCBS 077	15.50	0.00	30.00	54.50	cpb + E + Y	350	5	bm + E + Y

Solvent : 5 m NH_4Cl aqueous solution, * Silica tube was used as reaction vessel

$Cu_{8.4}Fe_{1.2}Bi_{10.8}S_{22}$, bismuthinite, and bismuth (liquid), were produced, but pyrite, covellite, and sulfur (liquid) did not appear in these runs, because the experiments under such high sulfur fugacity, as forming them, had not yet been performed. Also, emplectite was not found at this temperature. The phase relations in the quaternary system are shown in Fig. 11, but they are too complicated to be of any use in solving the phase diagram. Thus, the stable phase assemblages at 420°C are shown as the exploded diagram as Fig. 12. In the figure, heavy solid and dotted lines show the tie lines confirmed in the runs. Meanwhile, the tie lines expected are shown by light solid and dotted lines. As

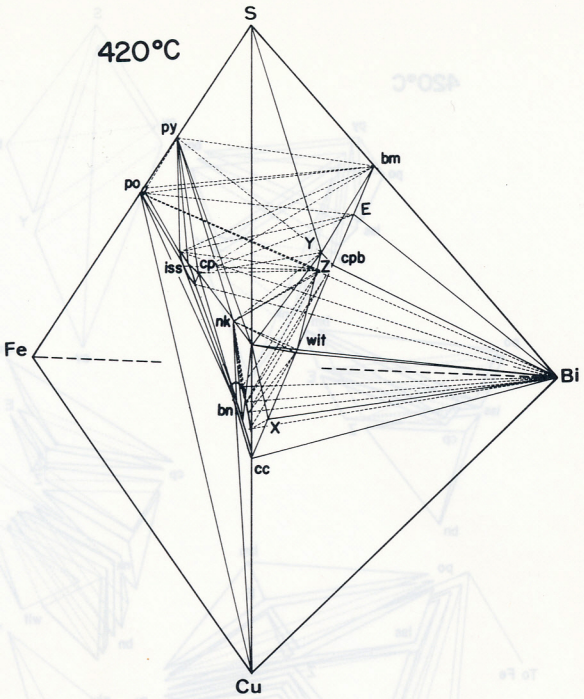

FIG. 11. Schematic phase diagram in the quaternary Cu–Fe–Bi–S system at 420°C under hydrothermal conditions.

seen in Fig. 12, the following univariant assemblages were recognized: bornite + phase Cu_9BiS_6 + wittichenite + bismuth (L), bornite + wittichenite + cuprobismutite + bismuth (L), bornite + cuprobismutite + phase $Cu_{8.4}Fe_{1.2}Bi_{10.8}S_{22}$ + bismuth (L), bornite + phase $Cu_{8.4}Fe_{1.2}Bi_{10.8}S_{22}$ + intermediate solid solution + bismuth (L), phase $Cu_{8.4}Fe_{1.2}Bi_{10.8}S_{22}$ + intermediate solid solution + pyrrhotite + bismuth (L), phase $Cu_{8.4}Fe_{1.2}Bi_{10.8}S_{22}$ + pyrrhotite + phase $CuBi_3S_5$ + bismuth (L), pyrrhotite + phase $CuBi_3S_5$ + bismuthinite + bismuth (L), cuprobismutite + phase $Cu_{8.4}Fe_{1.2}Bi_{10.8}S_{22}$ + phase $CuBi_3S_5$ + bismuth (L), (bornite + intermediate solid solution + pyrrhotite + bismuth (L))*, (bornite + pyrrhotite + copper + bismuth (L)), (pyrrhotite + copper + iron + bismuth (L)), (bornite + phase Cu_9BiS_6 + wittichenite + covellite), (bornite + wittichenite + covellite + nukundamite), (wittichenite + covellite + nukundamite + phase $Cu_8Bi_8S_{19}$), (wittichenite + cuprobismutite + phase $Cu_8Bi_8S_{19}$ + nukundamite), (bornite + wittichenite + cuprobismutite + nukundamite), bornite +

*The parentheses mean that the phase assemblage is inferred from experimental data.

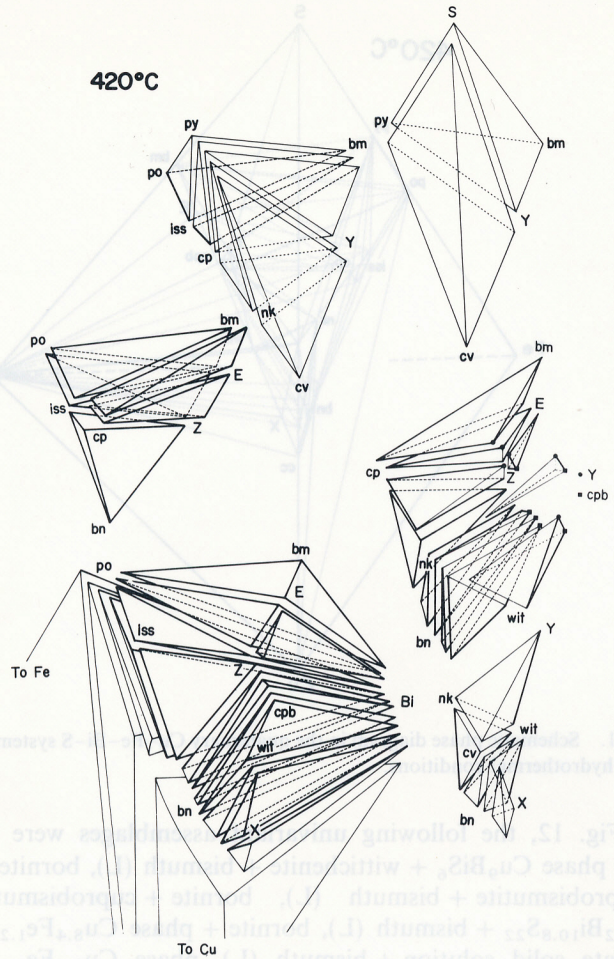

FIG. 12. Exploded phase diagram of phase relations in the system Cu–Fe–Bi–S at 420°C. Heavy solid and dot lines show the tie lines appeared in the hydrothermal experiments.

cuprobismutite + phase $Cu_{8.4}Fe_{1.2}Bi_{10.8}S_{22}$ + nukundamite, bornite + phase $Cu_{8.4}Fe_{1.2}Bi_{10.8}S_{22}$ + chalcopyrite + nukundamite, chalcopyrite + phase $Cu_{8.4}Fe_{1.2}Bi_{10.8}S_{22}$ + phase $Cu_8Bi_8S_{19}$ + nukundamite, cuprobismutite + phase $Cu_{8.4}Fe_{1.2}Bi_{10.8}S_{22}$ + phase $Cu_8Bi_8S_{19}$ + nukundamite, cuprobismutite + phase $Cu_{8.4}Fe_{1.2}Bi_{10.8}S_{22}$ + phase $Cu_8Bi_8S_{19}$ + phase $CuBi_3S_5$, chalcopyrite + phase $Cu_{8.4}Fe_{1.2}Bi_{10.8}S_{22}$ + phase $CuBi_3S_5$ + phase $Cu_8Bi_8S_{19}$, chalcopyrite + phase $CuBi_3S_5$ + bismuthinite + phase $Cu_8Bi_8S_{19}$, bornite + chalcopyrite + intermediate solid solution +

phase $Cu_{8.4}Fe_{1.2}Bi_{10.8}S_{22}$, chalcopyrite + intermediate solid solution + phase $Cu_{8.4}Fe_{1.2}Bi_{10.8}S_{22}$ + phase $CuBi_3S_5$, chalcopyrite + intermediate solid solution + bismuthinite + phase $CuBi_3S_5$, pyrrhotite + intermediate solid solution + bismuthinite + phase $CuBi_3S_5$, pyrrhotite + intermediate solid solution + phase $CuBi_3S_5$ + phase $Cu_{8.4}Fe_{1.2}Bi_{10.8}S_{22}$, (covellite + nukundamite + phase $Cu_8Bi_8S_{19}$ + pyrite), (chalcopyrite + nukundamite + phase $Cu_8Bi_8S_{19}$ + pyrite), (chalcopyrite + phase $Cu_8Bi_8S_{19}$ + bismuthinite + pyrite), (chalcopyrite + intermediate solid solution + bismuthinite + pyrite), (pyrrhotite + intermediate solid solution + bismuthinite + pyrite), (covellite + phase $Cu_8Bi_8S_{19}$ + pyrite + sulfur (L)), and (pyrite + bismuthinite + phase $Cu_8Bi_8S_{19}$ + sulfur (L)).

Phase $Cu_{8.4}Fe_{1.2}Bi_{10.8}S_{22}$ (Z), which is the only four-component phase in the quaternary system, occurs as a monoclinic polyhedral form, as shown in Fig. 3, though its appearance in nature is yet unknown. Its optical properties and X-ray powder data, lattice constants and DTA data were described in detail by SUGAKI *et al.* (1972, 1976a, 1981b). The crystal data of this phase is also summarized, together with other crystalline phases synthesized, in Table 1.

Among these phases, bornite, intermediate solid solution, wittichenite and cuprobismutite form some limited ranges of the solid solution. Thus, microprobe analyses were carried out on them and the coexisting phases with them. Results of the analyses are given in Table 3.

In order to make the phase relations clearly understandable, they can be presented in the triangle Cu–Fe–Bi plane by a projection from the sulfur summit to the metal basal plane in the tetrahedron of the quaternary system, as shown in Fig. 13. Figure 13-A shows the phase assemblages, which are produced under conditions of such comparatively higher sulfur fugacity as coexisting with nukundamite and phase $Cu_8Bi_8S_{19}$. On the other hand, Fig. 13-B represents the phase relations assembled with bismuth liquid, indicating a low sulfur fugacity condition. Bornite has a considerably wide space of solid solution and assembles stably with many phases, such as wittichenite, cuprobismutite, phase $Cu_{8.4}Fe_{1.2}Bi_{10.8}S_{22}$, chalcopyrite, intermediate solid solution, nukundamite and bismuth liquid. It does not associate with phase $CuBi_3S_5$, bismuthinite (and pyrite). While chalcopyrite coexists with phase $Cu_{8.4}Fe_{1.2}Bi_{10.8}S_{22}$, phase $CuBi_3S_5$, and bismuthinite, as well as the Cu–Fe–S minerals, the assemblage of chalcopyrite and wittichenite or cuprobismutite are not found. Wittichenite associates with cuprobismutite, phase $Cu_8Bi_8S_{19}$, bornite solid solution, nukundamite and bismuth liquid, but not with an assemblage of wittichenite with chalcopyrite, intermediate solid solution, phase $Cu_{8.4}Fe_{1.2}Bi_{10.8}S_{22}$, phase $CuBi_3S_5$, and bismuthinite. Cuprobismutite has the tie lines with bornite solid solution, nukundamite, wittichenite, phase $CuBi_3S_5$, phase $Cu_8Bi_8S_{19}$, phase $Cu_{8.4}Fe_{1.2}Bi_{10.8}S_{22}$, and bismuth liquid. Phase $Cu_{8.4}Fe_{1.2}Bi_{10.8}S_{22}$ (Z) appears in so stable a

TABLE 3. Analytical data for the phases synthesized by hydrothermal experimental runs at 420°C.

		Weight percent					Atomic percent				
	Phase	Cu	Fe	Bi	S	Total	Cu	Fe	Bi	S	Phase assemblage
HCFB 027	bn	53.1	8.5	13.9	23.6	99.1	46.7	8.5	3.7	41.1	bn + cpb
HCFB 028	cp	34.2	30.0	0.0	34.8	99.0	24.9	24.9	0.0	50.2	bn + cp + Z
HCFB 038	bn	52.2	12.1	10.5	25.2	100.0	43.6	11.4	2.7	42.3	bn + cpb + Z
	Z	15.4	1.4	63.1	19.9	99.8	20.4	2.1	25.4	52.2	
HCFB 043	cpb	15.5	0.3	64.0	19.3	99.1	21.1	0.5	26.5	51.9	bn + cpb
HCFB 044	Z	14.6	1.5	64.6	19.9	100.6	19.4	2.3	26.1	52.3	bn + cp + nk + Z
HCFB 045	cp	34.2	30.5	0.0	34.6	99.3	24.9	25.2	0.0	49.9	cp + bm + E + Y
	bm	0.9	0.4	79.6	19.0	99.9	1.5	0.8	38.2	59.6	
HCFB 046	bn	63.0	6.0	7.5	23.7	100.2	53.0	5.7	1.9	39.5	bn + wit
	wit	36.5	0.0	44.9	19.3	100.7	41.3	0.0	15.4	43.3	
HCFB 047	bn	54.5	7.0	13.8	23.8	99.1	47.9	7.0	3.7	41.4	bn + cpb + wit
	cpb	15.5	0.5	64.7	19.0	99.7	21.1	0.8	26.8	51.3	
	wit	37.1	0.1	42.4	19.3	98.9	42.1	0.1	14.6	43.3	
HCFB 048	cp	34.0	30.4	0.0	34.8	99.2	24.7	25.1	0.0	50.2	cp + Z + E
	E	7.2	0.2	73.6	19.2	100.2	10.6	0.3	33.0	56.1	
HCFB 053	bn	48.1	13.7	11.3	26.4	99.5	40.3	13.1	2.9	43.8	bn + Z
	Z	15.1	1.4	63.7	19.5	99.7	20.2	2.1	25.9	51.8	
HCFB 077	wit	36.4	0.1	44.4	18.9	99.8	41.6	0.1	15.4	42.8	wit + cpb + Bi
	cpb	15.4	0.1	66.0	19.0	100.6	21.1	0.2	27.4	51.3	
HCFB 078	E	8.4	0.0	74.2	18.9	101.5	12.3	0.0	33.0	54.7	E
HCFB 079	wit	36.0	0.3	44.5	19.5	100.3	40.7	0.4	15.3	43.7	wit + Bi
HCFB 089	bn	43.9	16.3	12.9	27.3	100.4	36.4	15.4	3.3	44.9	bn + Bi
HCFB 090	bn	37.0	17.6	17.2	27.2	99.6	31.6	17.1	4.5	46.9	bn + iss + Bi
	iss	31.6	32.9	1.9	34.5	100.9	22.9	27.2	0.4	49.6	
HCFB 091	bn	39.4	17.2	15.2	27.4	99.2	33.4	16.6	3.9	46.0	bn + Bi
HCFB 092	iss	27.8	37.4	0.4	34.8	100.4	19.9	30.5	0.1	49.5	iss + po + Bi
	po	0.7	62.1	0.0	37.2	100.0	0.5	48.7	0.0	50.8	
HCFB 093	bn	52.3	13.3	9.2	25.2	100.1	43.5	12.6	2.3	41.6	bn + wit + Bi
	wit	36.4	0.1	45.2	19.2	100.9	41.2	0.1	15.6	43.1	
HCFB 094	bn	52.3	13.8	10.1	24.6	100.8	43.6	13.1	2.6	40.7	bn + wit + Bi
	wit	35.7	0.3	44.8	18.9	99.7	40.9	0.4	15.6	43.0	
HCFB 095	bn	49.4	14.2	10.9	26.5	101.0	40.7	13.3	2.7	43.3	bn + Bi
HCFB 096	bn	50.0	14.0	12.0	25.2	101.2	41.8	13.3	3.1	41.8	bn + wit + Bi
HCFB 107	iss	23.3	40.6	0.2	35.4	99.5	16.7	33.1	0.0	50.2	iss + po + Bi
	po	0.7	61.3	0.3	38.0	100.3	0.5	47.8	0.1	51.6	
HCFB 108	wit	39.7	0.1	42.4	18.4	100.6	44.5	0.1	14.5	40.9	wit + X + Bi
	X	59.7	0.1	21.2	19.0	100.0	57.4	0.1	6.2	36.2	
HCFB 109	E	8.7	0.3	72.3	18.8	100.1	12.7	0.5	32.2	54.6	po + E
HCFB 123	bn	43.4	16.2	15.1	26.5	101.2	36.5	15.5	3.9	44.2	bn + Z + Bi
	Z	13.1	2.3	66.0	19.5	100.9	17.6	3.5	27.0	51.9	
HCFB 125	wit	38.2	0.1	41.8	19.2	99.3	42.9	0.1	14.3	42.7	wit + X + Bi
HCFB 126	X	57.8	0.2	22.3	19.9	100.2	55.4	0.2	6.5	37.8	bn + X + Bi
HCFB 128	bn	48.1	15.1	12.5	25.7	101.4	40.1	14.3	3.2	42.4	bn + Z + Bi
	Z	14.2	2.3	63.0	19.6	99.1	19.0	3.5	25.6	51.9	
HCFB 132	E	8.7	0.2	72.3	18.8	100.0	12.8	0.3	32.2	54.7	cpb + E + Bi
	cpb	15.1	0.1	65.9	19.0	100.1	20.7	0.2	27.5	51.7	

form as to coexist with a lot of phases, such as bornite solid solution, intermediate solid solution, chalcopyrite, nukundamite, cuprobismutite, phase $CuBi_3S_5$, phase $Cu_8Bi_8S_{19}$, and bismuth liquid. Bismuthinite assembles with chalcopyrite, intermediate solid solution, pyrrhotite, phase $CuBi_3S_5$, phase $Cu_8Bi_8S_{19}$, bismuth liquid, and pyrite.

The bornite solid solution at 420°C contains considerable quantities of iron and bismuth. A composition of bornite, which nearly corresponds to the maximum contents of iron and bismuth, is Cu 37.0, Fe 17.6, Bi 17.2, and S 27.2 in weight percent, as is presented in the chemical formula $Cu_{3.16}Fe_{1.71}Bi_{0.45}S_{4.69}$ as the total atomic number ten. It associates with

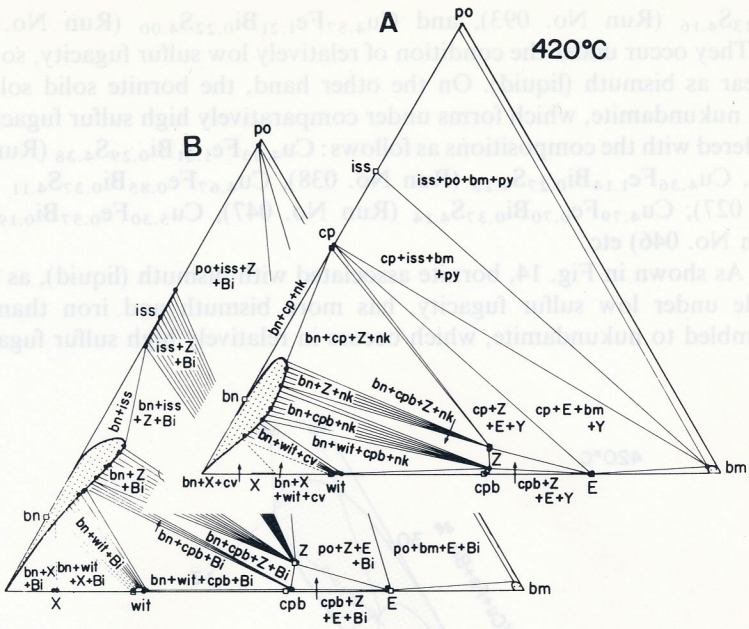

FIG. 13. Phase relations of relatively sulfur-rich (A) and metal rich (B) parts of the Cu–Fe–Bi–S system at 420°C obtained by projection from sulfur corner to the basal Cu–Fe–Bi plane in the tetrahedron of the quaternary Cu–Fe–Bi–S.

intermediate solid solution and bismuth liquid, as given in Table 3 (Run No. 090), very close to the point of univariant assemblage with intermediate solid solution and phase $Cu_{8.4}Fe_{1.2}Bi_{10.8}S_{22}$, approached at a univariant point of the association with chalcopyrite, phase $Cu_{8.4}Fe_{1.2}Bi_{10.8}S_{22}$, and nukundamite, and has Cu 48.1, Fe 13.7, Bi 11.3, and S 26.4 in a weight percent corresponding to $Cu_{4.03}Fe_{1.31}Bi_{0.29}S_{4.38}$ (Run No. 053 in Table 3). Also bornite, which assembles with wittichenite and bismuth liquid, got very near to a univariant point of the assemblage with wittichenite, cuprobismutite, and bismuth liquid and contains Cu 52.3, Fe 13.8, Bi 10.1, and S 24.6 in weight percent ($Cu_{4.36}Fe_{1.31}Bi_{0.26}S_{4.07}$). Meanwhile, the composition of bornite with wittichenite and cuprobismutite, get very close to the univariant point of the association of bornite + wittichenite + cuprobismutite + nukundamite and is Cu 54.5, Fe 7.0, Bi 13.8, and S 23.8 in weight percent ($Cu_{4.79}Fe_{0.70}Bi_{0.37}S_{4.14}$). The bornite solid solution compositions in equilibrium with bismuth liquid along the boundary at 420°C are, in order of bismuth-richness, as follows: $Cu_{3.16}Fe_{1.71}Bi_{0.45}S_{4.69}$ (Run No. 090) $Cu_{3.64}Fe_{1.54}Bi_{0.33}S_{4.49}$ (Run No. 089), $Cu_{3.79}Fe_{1.50}Bi_{0.35}S_{4.36}$ (Run No. 130), $Cu_{4.01}Fe_{1.43}Bi_{0.32}S_{4.24}$ (Run No. 128), $Cu_{4.07}Fe_{1.33}Bi_{0.27}S_{4.33}$ (Run No. 095), $Cu_{4.36}Fe_{1.31}Bi_{0.26}$ $S_{4.07}$ (Run No. 094), $Cu_{4.35}Fe_{1.26}$

$Bi_{0.23}S_{4.16}$ (Run No. 093), and $Cu_{4.57}Fe_{1.21}Bi_{0.22}S_{4.00}$ (Run No. 133) etc. They occur under the condition of relatively low sulfur fugacity, so as to appear as bismuth (liquid). On the other hand, the bornite solid solution with nukundamite, which forms under comparatively high sulfur fugacity, is bordered with the compositions as follows: $Cu_{4.03}Fe_{1.31}Bi_{0.29}S_{4.38}$ (Run No. 053), $Cu_{4.36}Fe_{1.14}Bi_{0.27}S_{4.23}$ (Run No. 038), $Cu_{4.67}Fe_{0.85}Bi_{0.37}S_{4.11}$ (Run No. 027), $Cu_{4.79}Fe_{0.70}Bi_{0.37}S_{4.14}$ (Run No. 047), $Cu_{5.30}Fe_{0.57}Bi_{0.19}S_{3.95}$ (Run No. 046) etc.

As shown in Fig. 14, bornite associated with bismuth (liquid), as to be stable under low sulfur fugacity, has more bismuth and iron than one assembled to nukundamite, which occurs in relatively high sulfur fugacity.

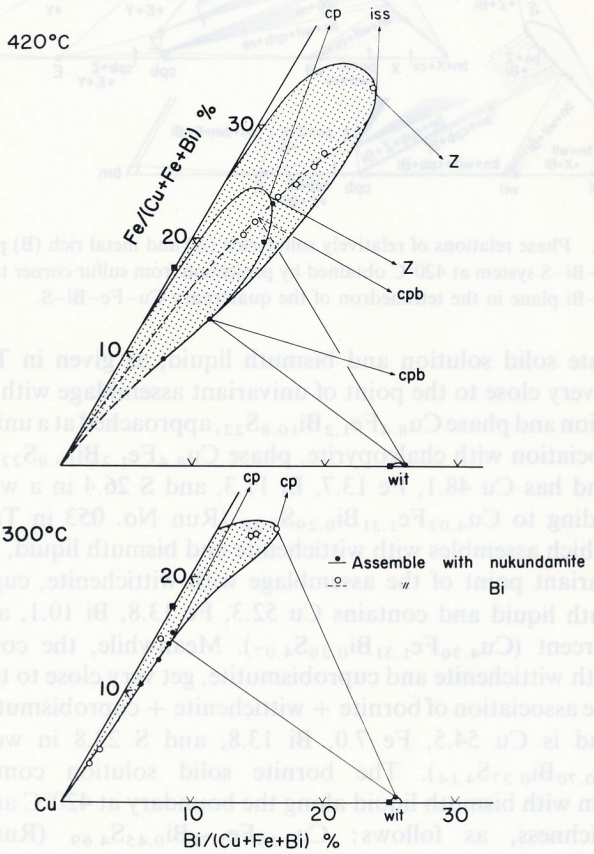

FIG. 14. The area of bornite solid solution at 420° and 300°C. Open circle show the composition of bornite associated with bismuth liquid, while solid one, bornite with nukundamite.

3.4.2 The phase relations at 300°C

The results of the experiments at 300°C are given in Table 4. The phases produced at 300°C are almost the same as 420°C except that emplectite appears instead of cuprobismutite. Phase relations in the quaternary system at 300°C are shown in Fig. 15, but this figure is complicated. Thus, in order to solve the phase relations the figure was simplified, as Fig. 16. This figure shows the phase relations of the quaternary system at 300°C presented by projection from the sulfur corner to the basal Cu–Fe–Bi plane of the tetrahedron Cu–Fe–Bi–S. The stable phase assemblages under conditions of comparatively high sulfur fugacity, so as to coexist with nukundamite and phase $Cu_8Bi_8S_{19}$, are given in Fig. 16-A, while the phase relations under low sulfur fugacity with bismuth (liquid) are shown in Fig. 16-B. As found in Fig. 16, the association of chalcopyrite and wittichenite appears instead of the assemblages of bornite + cuprobismutite and bornite + phase $Cu_{8.4}Fe_{1.2}Bi_{10.8}S_{22}$ at 420°C. The univariant assemblages of bornite + chalcopyrite + wittichenite + nukundamite or bismuth liquid, chalcopyrite + wittichenite + phase $Cu_{8.4}Fe_{1.2}Bi_{10.8}S_{22}$ + nukundamite or bismuth liquid, and wittichenite + emplectite + phase $Cu_{8.4}Fe_{1.2}Bi_{10.8}S_{22}$ + phase $Cu_8Bi_8S_{19}$ or bismuth liquid become stable. In addition to them, the following univariant assemblages in the quaternary system at 300°C are found in Fig. 17 shown as a decomposed diagram of the quaternary tetrahedron in Fig. 15. Chalcopyrite + phase $Cu_{8.4}Fe_{1.2}Bi_{10.8}S_{22}$ + phase $CuBi_3S_5$ + bismuth (L), chalcopyrite + phase $CuBi_3S_5$ + bismuthinite + bismuth (L), chalcopyrite + intermediate solid solution + bismuthinite + bismuth (L), pyrrhotite + intermediate solid solution + bismuthinite + bismuth (L), emplectite + phase $Cu_{8.4}Fe_{1.2}Bi_{10.8}S_{22}$ + phase $CuBi_3S_5$ + bismuth (L), (bornite + chalcopyrite + intermediate solid solution + bismuth (L)), (bornite + intermediate solid solution + pyrrhotite + bismuth (L)), (bornite + pyrrhotite + copper + bismuth (L)), (pyrrhotite + copper + iron + bismuth (L)), (bornite + wittichenite + nukundamite + covellite), (covellite + wittichenite + nukundamite + phase $Cu_8Bi_8S_{19}$), wittichenite + nukundamite + phase $Cu_{8.4}Fe_{1.2}Bi_{10.8}S_{22}$ + phase $Cu_8Bi_8S_{19}$, chalcopyrite + nukundamite + phase $Cu_{8.4}Fe_{1.2}Bi_{10.8}S_{22}$ + phase $Cu_8Bi_8S_{19}$, chalcopyrite + phase $CuBi_3S_5$ + phase $Cu_{8.4}Fe_{1.2}Bi_{10.8}S_{22}$ + phase $Cu_8Bi_8S_{19}$, chalcopyrite + bismuthinite + phase $CuBi_3S_5$ + phase $Cu_8Bu_8S_{19}$, chalcopyrite + intermediate solid solution + pyrrhotite + bismuthinite, emplectite + phase $Cu_{8.4}Fe_{1.2}Bi_{10.8}S_{22}$ + phase $CuBi_3S_5$ + phase $Cu_8Bi_8S_{19}$, (covellite + nukundamite + phase $Cu_8Bi_8S_{19}$ + pyrite), (chalcopyrite + nukundamite + phase $Cu_8Bi_8S_{19}$ + pyrite), (chalcopyrite + bismuthinite + phase $Cu_8Bi_8S_{19}$ + pyrite), (chalcopyrite + pyrrhotite + bismuthinite + pyrite), (covellite + phase $Cu_8Bi_8S_{19}$ + pyrite + sulfur (L)), and (bismuthinite + phase $Cu_8Bi_8S_{19}$ + pyrite + sulfur (L)).

Emplectite, which first appears at 300°C, can coexist with wittichenite,

TABLE 4. Hydrothermal experimental results at 300°C in the Cu–Fe–Bi–S system.

Run No.	Nutrient materials: Composition (Atomic %) Cu	Fe	Bi	S	Reactants	Pressure (kg/cm^2)	Heating period (days)	Synthesized phases
HCFB 002	39.33	4.91	11.48	44.48	bn + wit + Z	395	8	bn + cp + wit
HCFB 004	32.64	14.28	6.12	46.96	bn + cp + Bi	412	11	bn + cp + wit
HCFB 005	40.59	3.13	12.50	43.78	bn + wit + Bi	412	11	bn + cp + wit
HCFB 006	30.42	17.39	4.35	47.84	bn + cp + Z	412	11	cp + wit + nk + Z
HCFB 007	36.35	9.10	9.90	45.47	bn + Z	396	10	cp + wit + nk
HCFB 008	34.61	11.54	7.69	46.16	bn + cp + Z	396	10	cp + wit + nk + Z
HCFB 009	44.74	2.63	10.53	42.10	bn + wit	400	11	bn + cp + wit
HCFB 010	46.33	4.88	7.31	41.47	bn + wit	400	11	bn + wit
HCFB 011	47.74	6.80	4.55	40.91	bn	410	13	bn + cp + wit
HCFB o12	48.94	8.51	2.14	40.42	bn	410	13	bn + cp + Bi
HCFB 014	24.99	12.50	12.50	50.01	bn + cp + Z	420	10	cp + wit + Z
HCFB 015	15.05	0.77	30.20	53.98	D + E + Z	385	13	emp + E + Z + Y
HCFB 016	20.14	1.01	26.92	51.92	wit + D + E	385	13	emp + E + Z
HCFB 018	24.98	4.22	20.80	50.00	bn + wit + Z	390	13	cp + Z + Y
HCFB 019	19.12	2.87	25.69	52.32	cp + Z	380	9	cp + wit + Z
HCFB 020	16.46	6.32	23.83	53.40	cp + E + Z	380	9	cp + Z + Y
HCFB 021	45.62	4.81	8.64	40.92	bn + wit + Bi	395	9	bn + cp
HCFB 023	24.99	6.45	18.56	50.00	bn + Z	395	8	cp + Z + Y
HCFB 024	24.59	6.32	19.81	49.28	bn + Z + Bi	395	8	bn + cp + wit + nk
HCFB 025	16.51	30.82	5.50	47.17	wit + po	410	14	iss + Bi
HCFB 026	23.03	23.20	7.68	46.09	wit + po	410	14	cp + Z
HCFB 033	40.21	10.98	4.87	43.94	bn + cp + wit	400	25	cp + wit
HCFB 044	16.51	30.82	5.50	47.17	wit + po	400	25	iss + bm + Bi
HCFB 035	20.80	25.55	6.94	46.72	wit + po	410	25	iss + po + bm + Bi
HCFB 036	27.24	18.29	9.08	45.39	wit + po	410	25	cp + wit + Bi
HCFB 041	8.05	13.79	24.12	54.04	po + E	400	21	iss + po + bm + Bi
HCFB 042	5.33	26.03	15.97	52.67	po + E	400	21	po + bm
HCFB 070 *	7.68	1.41	60.77	30.13	iss + E + Bi	300	7	bm + E + Bi
HCFB 073 *	17.47	1.48	51.01	30.05	bn + cpb + Bi	300	10	bn + cp + Bi
HCFB 074 *	24.49	3.49	41.99	30.03	bn + cpb + Bi	300	10	cp + wit + Bi
HCFB 083 *	10.50	3.49	56.02	29.99	iss + Z + Bi	300	21	bn + cp + Bi
HCFB 084 *	17.48	17.53	34.97	30.02	bn + iss + Bi	300	21	cp + Z + Bi
HCFB 085 *	14.99	17.50	37.48	30.02	iss + Bi	300	21	bn + cp + Bi
HCFB 086 *	12.49	17.52	39.97	30.02	iss + Bi	300	21	iss + bm + Bi
HCFB 087 *	22.47	14.02	33.47	30.04	bn + iss + Bi	300	19	bn + cp + Bi
HCFB 088 *	15.99	14.98	38.99	30.04	bn + iss + Z + Bi	300	19	cp + wit + Bi
HCFB 097 *	44.96	1.40	23.60	30.04	bn + X + Bi	300	18	bn + wit + Bi
HCFB 098 *	20.99	10.52	38.49	30.00	bn + iss + Z + Bi	300	18	cp + wit + Bi
HCFB 099 *	10.00	22.50	37.51	29.99	iss + po + Bi	300	18	iss + Bi
HCFB 100 *	6.99	7.00	55.95	30.06	iss + Z + Bi	300	18	cp + bm + Bi
HCFB 101 *	33.57	1.39	34.96	30.08	bn + wit + Bi	300	18	bn + wit + Bi
HCFB 102 *	5.00	22.48	42.48	30.04	iss + po + bm + Bi	300	18	iss + po + bm + Bi
HCFB 103 *	24.47	7.01	38.45	30.07	bn + Z + Bi	300	18	bn + cp + wit + Bi
HCFB 104 *	21.00	6.98	42.00	30.02	bn + Z + Bi	300	18	cp + Bi
HCFB 105 *	17.48	10.54	41.98	30.01	bn + iss + Z + Bi	300	18	cp + wit + Bi
HCFB 114 *	10.50	10.51	49.00	29.99	iss + bm + E + Bi	300	18	cp + bm + Bi
HCFB 115 *	14.00	7.02	49.00	29.99	bn + iss + Z + Bi	300	18	cp + bm + Bi
HCFB 117 *	30.09	1.34	38.49	30.08	bn + wit + cpb + Bi	300	18	cp + wit + Bi
HCFB 118 *	19.99	14.01	35.98	30.02	bn + iss + Bi	300	18	bn + cp + wit + Bi
HCFB 119 *	10.14	13.51	47.32	29.03	iss + Z + Bi	300	18	cp + bm + Bi
HCFB 121 *	13.51	13.53	43.90	29.05	bn + iss + Z + Bi	300	18	cp + Bi
HCFB 122 *	16.90	13.54	40.57	28.97	bn + iss + Z + Bi	300	18	cp + wit + Bi
HCBF 003	19.70	3.00	25.50	51.80	cp + Z	300	10	cp + Z
HCBS 069	28.20	0.00	23.08	48.72	wit + cpb	300	13	emp + wit
HCBS 084	18.82	0.00	28.23	52.94	cpb + E	280	21	wit + emp + Y
HCBS 095	15.50	0.00	30.00	54.50	cpb + E + Y	350	15	bm + E + Y

Solvent : 5 m NH_4Cl aqueous solution, * Silica tube was used as reaction vessel

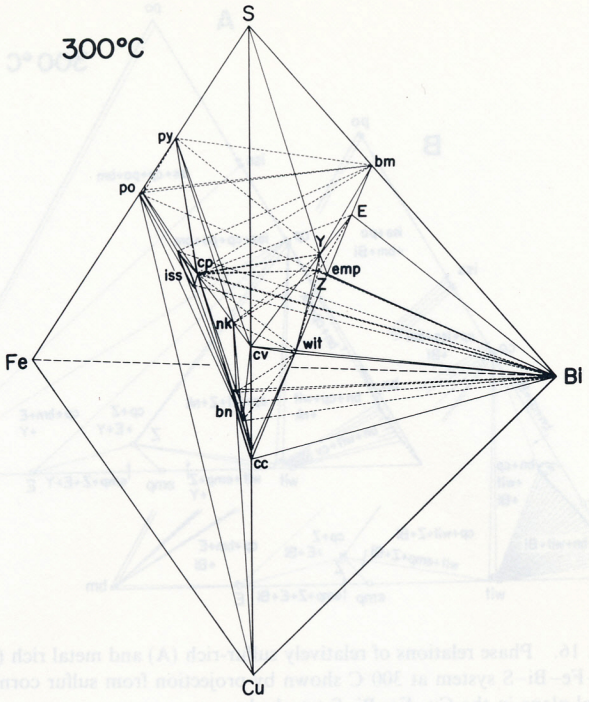

FIG. 15. Schematic diagram in the quaternary Cu–Fe–Bi–S system at 300°C under hydrothermal conditions.

phase $CuBi_3S_5$, phase $Cu_8Bi_8S_{19}$, phase $Cu_{8.4}Fe_{1.2}Bi_{10.8}S_{22}$, nukundamite, and bismuth liquid, but it cannot associate with bornite, chalcopyrite, intermediate solid solution, pyrrhotite, and bismuthinite, etc., although it occurs in intimate association with bornite, chalcopyrite, and bismuthinite in natural copper-bismuth ores.

Analytical data for the solid phases synthesized in each run by microprobe analyser are given in Table 5. As seen in the table, bornite still has a passable space of the solid solution although it becomes smaller in comparison with that at 420°C. Bornite, which occurs just as a univariant assemblage with chalcopyrite, wittichenite, and bismuth liquid, has the composition of Cu 47.8, Fe 14.4, Bi 11.4, and S 25.9 in weight percent corresponding to the formula $Cu_{4.02}Fe_{1.37}Bi_{0.29}S_{4.32}$ (Run No. 103). This composition is nearly the maximum content of iron and bismuth at 300°C, while bornite with chalcopyrite and wittichenite, close to a univariant point of the assemblage bornite + chalcopyrite + wittichenite + nukundamite, contains Cu 63.6, Fe 9.2, Bi 3.4, and S 24.1 in weight percent corresponding to $Cu_{5.18}Fe_{0.85}Bi_{0.08}S_{3.89}$ (Run No. 011). The same as at

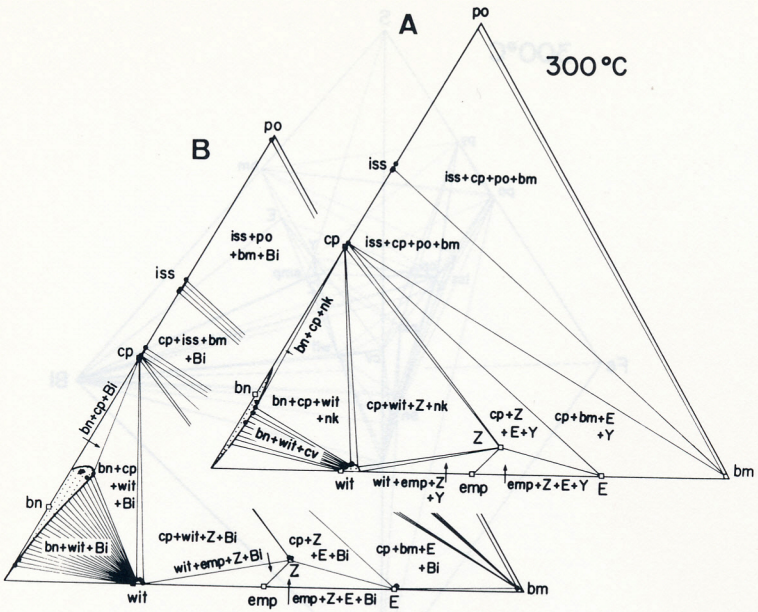

FIG. 16. Phase relations of relatively sulfur-rich (A) and metal rich (B) parts of the Cu–Fe–Bi–S system at 300°C shown by projection from sulfur corner to the basal metal plane in the Cu–Fe–Bi–S tetrahedron.

420°C, bornite with bismuth (liquid) also contains more iron and bismuth than bornite with nukundamite, as shown in Fig. 14. Wittichenite has a very limited range of solid solution at 300°C from Cu_3BiS_3 to $Cu_{2.83}Bi_{1.10}S_{3.07}$ in the binary Cu_2S–Bi_2S_3, as reported by SUGAKI and SHIMA (1971, 1972b), and includes 0.6 to 1.0 weight percent iron (0.8 to 1.3 atomic percent iron) in the case associated with chalcopyrite. Emplectite and phase $CuBi_3S_5$ almost contain no iron. Intermediate solid solution has very small amounts of bismuth, 0.9 weight percent or less, and chalcopyrite also contains only 0.2 weight percent or less.

4. *Discussion*

4.1 *Bornite solid solution*

As mentioned above, bornite synthesized hydrothermally in the Cu–Fe–Bi–S system has a relatively extensive field of solid solution, containing a maximum of 17.2 weight percent bismuth at 420°C. Similarly, NANRI *et al.* (1978) carried out experiments on the system Cu–Fe–Bi–S using the dry method, and reported that bornite solid solution appeared in a large area, having a maximum of 18.2 weight percent bismuth at 500°C. Bornite

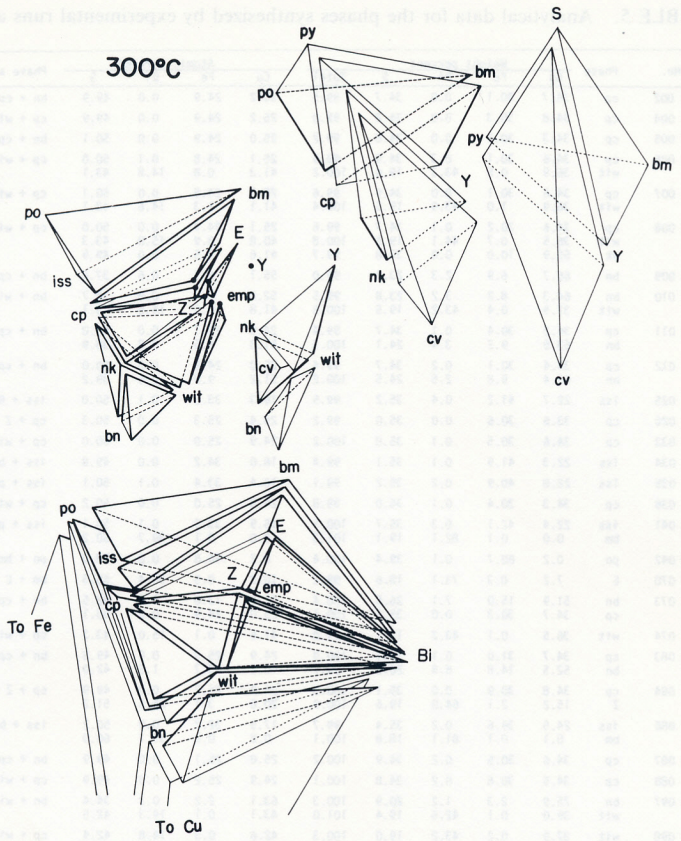

FIG. 17. Exploded phase diagrams showing stable phase assemblages in the Cu–Fe–Bi–S system at 300°C.

forms a fairly wider solid solution under low sulfur fugacity condition, as coexisting with bismuth (liquid), than its field under a high sulfur fugacity accompanied by unkundamite at constant temperatures, as shown in Fig. 14. The bornite solid solution in the quaternary system becomes more iron-and sulfur-rich besides bismuth than it does in the system Cu–Fe–S, as shown in Fig. 18 which shows the bornite solid solution by projection on the Cu–Fe–S plane from the bismuth corner of the tetrahedron, and contains 14.4 and 17.6 weight percent iron, and 25.9 and 27.2 weight percent sulfur in maximum at 300° and 420°C, respectively. Figure 18 shows a field of bornite solid solution at 420°C in comparison with that of bornite at 400°C in the system Cu–Fe–S. Bornite, which is mostly iron-and sulfur-rich, is produced in the case coexisting with phase $Cu_{8.4}Fe_{1.2}Bi_{10.8}S_{22}$ (Z), and the iron and sulfur contents in the bornite solid solution decrease in order of phase assemblage

TABLE 5. Analytical data for the phases synthesized by experimental runs at 300°C.

Run No.	Phase	Weight percent					Atomic percent				Phase assemblage
		Cu	Fe	Bi	S	Total	Cu	Fe	Bi	S	
HCFB 002	cp	34.7	30.1	0.0	34.7	99.5	25.2	24.9	0.0	49.9	bn + cp + wit
HCFB 004	cp	34.8	30.3	0.0	34.8	99.0	25.2	24.9	0.0	49.9	cp + wit + bn
HCFB 005	cp	34.3	30.1	0.0	34.8	99.2	25.0	24.9	0.0	50.1	bn + cp + wit
HCFB 006	cp	34.6	30.1	0.3	34.9	99.9	25.1	24.8	0.1	50.0	cp + wit + nk + Z
	wit	36.9	0.6	43.3	19.4	100.2	41.3	0.8	14.8	43.1	
HCFB 007	cp	34.6	30.1	0.0	34.9	99.6	25.1	24.8	0.0	50.1	cp + wit + nk
	wit	36.9	1.0	43.0	19.5	100.4	41.1	1.3	14.6	43.1	
HCFB 008	cp	34.6	30.2	0.1	34.7	99.6	25.1	24.9	0.0	50.0	cp + wit + nk + Z
	wit	36.5	0.7	44.1	19.5	100.8	40.8	0.9	15.0	43.3	
	nk	55.9	10.0	0.0	33.8	99.7	41.6	8.5	0.0	49.9	
HCFB 009	bn	66.7	6.9	2.3	23.1	99.0	55.1	6.5	0.6	37.8	bn + cp + wit
HCFB 010	bn	64.3	8.2	3.2	23.8	99.5	52.8	7.7	0.8	38.7	bn + wit
	wit	37.5	0.4	43.2	19.5	100.6	41.8	0.5	14.6	43.1	
HCFB 011	cp	34.2	30.4	0.1	34.7	99.4	24.9	25.1	0.0	50.0	bn + cp + wit
	bn	63.6	9.2	3.4	24.1	100.3	51.8	8.5	0.8	38.9	
HCFB 012	cp	34.4	30.1	0.2	34.7	99.4	25.0	24.9	0.0	50.0	bn + cp + Bi
	bn	63.4	9.8	2.5	24.5	100.2	51.2	9.0	0.6	39.2	
HCFB 025	iss	22.7	41.2	0.4	35.2	99.5	16.3	33.6	0.1	50.0	iss + Bi
HCFB 026	cp	33.6	30.6	0.0	35.0	99.2	24.4	25.3	0.0	50.3	cp + Z
HCFB 033	cp	34.6	30.5	0.1	35.0	100.2	24.9	25.0	0.0	50.0	cp + wit
HCFB 034	iss	22.3	41.9	0.1	35.1	99.4	16.0	34.2	0.0	49.8	iss + bm + Bi
HCFB 035	iss	22.8	40.9	0.2	35.2	99.1	16.4	33.4	0.1	50.1	iss + po + bm + Bi
HCFB 036	cp	34.3	30.4	0.1	35.0	99.8	24.8	25.0	0.0	50.2	cp + wit + Bi
HCFB 041	iss	22.4	42.1	0.3	35.7	100.5	15.9	33.9	0.1	50.1	iss + po + bm + Bi
	bm	0.0	0.1	82.1	19.1	101.3	0.0	0.1	39.7	60.2	
HCFB 042	po	0.2	60.7	0.1	39.4	100.4	0.2	46.8	0.0	53.0	po + bm
HCFB 070	E	7.2	0.3	73.1	18.6	99.2	10.8	0.5	33.4	55.3	bm + E + Bi
HCFB 073	bn	51.9	15.0	7.1	26.5	100.4	42.0	13.8	1.8	42.5	bn + cp + Bi
	cp	34.7	30.3	0.0	35.1	100.1	25.0	24.9	0.0	50.1	
HCFB 074	wit	36.5	0.1	43.2	19.2	99.0	41.6	0.1	15.0	43.3	cp + wit + Bi
HCFB 083	cp	34.7	31.0	0.1	35.1	100.9	24.9	25.3	0.0	49.8	bn + cp + Bi
	bn	52.5	14.8	6.4	26.0	99.7	42.8	13.7	1.6	42.0	
HCFB 084	cp	34.8	30.9	0.0	35.1	100.8	24.9	25.2	0.0	49.9	cp + Z + Bi
	Z	15.2	2.1	64.0	19.6	100.9	20.0	3.1	25.6	51.2	
HCFB 086	iss	24.5	39.6	0.2	35.4	99.7	17.5	32.2	0.0	50.2	iss + bm + Bi
	bm	0.1	0.1	81.1	18.8	100.1	0.2	0.2	39.7	60.0	
HCFB 087	cp	34.6	30.5	0.2	34.9	100.2	25.0	25.1	0.0	49.9	bn + cp + Bi
HCFB 088	cp	34.5	30.6	0.2	34.8	100.1	24.9	25.2	0.0	49.9	cp + wit + Bi
HCFB 097	bn	75.9	2.3	1.2	20.9	100.3	63.1	2.2	0.3	34.4	bn + wit + Bi
	wit	39.0	0.1	42.5	19.4	101.0	43.1	0.1	14.3	42.5	
HCFB 098	wit	37.9	0.2	43.2	19.0	100.3	42.6	0.3	14.8	42.4	cp + wit + Bi
	cp	34.5	30.4	0.2	34.7	99.8	25.0	25.1	0.0	49.9	
HCFB 099	iss	24.2	40.2	0.1	35.5	100.0	17.2	32.6	0.0	50.1	iss + Bi
HCFB 100	bm	1.4	0.5	79.4	18.5	99.8	2.2	0.9	38.5	58.4	cp + bm + Bi
HCFB 101	bn	74.5	3.3	1.6	21.6	101.0	61.3	3.1	0.4	35.2	bn + wit + Bi
HCFB 102	iss	22.4	41.7	0.9	35.5	100.5	16.0	33.8	0.2	50.1	iss + po + bm + Bi
	po	0.2	61.3	0.3	38.6	100.4	0.1	47.6	0.1	52.2	
	bm	0.1	0.1	80.9	18.5	99.6	0.2	0.2	40.0	59.6	
HCFB 103	bn	47.8	14.4	11.4	25.9	99.5	40.2	13.7	2.9	43.2	bn + cp + wit + Bi
	wit	38.6	0.4	42.5	19.2	100.7	42.9	0.5	14.4	42.3	
HCFB 119	cp	33.2	32.0	0.2	35.1	100.4	23.8	26.1	0.0	49.9	cp + bm + Bi
	bm	0.1	0.1	81.6	18.6	100.4	0.2	0.2	40.1	59.6	
HCFB 003	Z	14.9	1.8	63.3	19.9	99.9	19.7	2.7	25.4	52.1	cp + Z
HCBS 069	wit	36.1	0.0	44.3	19.7	100.1	40.7	0.0	15.2	44.1	emp + wit
	emp	18.8	0.0	61.9	19.0	99.7	25.0	0.0	25.0	50.0	
HCBS 095	E	7.7	0.0	73.5	19.2	100.4	11.3	0.0	32.8	55.9	bm + E + Y

with cuprobismutite and wittichenite, as seen in the figure. The upper curve bordering the bornite solid solution represents the solvus of the solid solution associating with the phases having a comparatively high sulfur fugacity, such as nukundamite and phase $Cu_8Bi_8S_{19}$. The low curve corresponds to the solvus associating with bismuth liquid, which is stable under low sulfur fugacity. Although it can contain more bismuth, iron, and sulfur than its

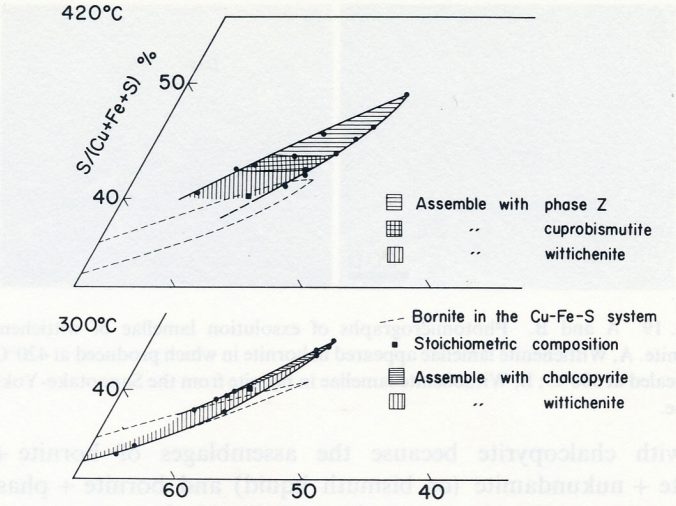

FIG. 18. The regions of bornite solid solution at 420° and 300°C obtained by projection from bismuth corner to Cu–Fe–S plane in the tetrahedron. The areas of bornite solid solution under hydrothermal conditions in the Cu–Fe–S system are also shown together.

stoichiometric composition at high temperatures, bornite in natural ores has a stoichiometric composition with no bismuth, as reported by SUGAKI *et al.* (1973). Thus, it is a possibility that bornite in bismuth-bearing copper ores, formed at higher temperature than about 300°C, exsolves bismuth minerals such as wittichenite during cooling. In fact, wittichenite (klaprothite) occasionally occurs as exsolution lamella in natural bornite, as described by WATANABE (1937, 1951) and KRIEGER (1940). In order to experimentally confirm the exsolution of bismuth minerals from bornite solid solution, bornite with Cu 54.5, Fe 7.0, Bi 13.8, and S 23.8 in weight percent ($Cu_{4.79}Fe_{0.70}Bi_{0.37}S_{4.14}$) which was synthesized hydrothermally at 420°C, was annealed at 300°C for 12 hours under a pyrrhotite (48.0 atomic percent iron) buffer. Consequently it is found that wittichenite is exsoluted as lamella in bornite, as shown in Fig. 19-A. In this figure (Fig. 19-B) exsolution lamella of wittichenite in bornite from Sannotake-Yokozuru mine, Fukuoka prefecture, Japan, is shown in comparison with the experimental product above.

4.2 *Chalcopyrite and wittichenite assemblage*

Chalcopyrite and bornite occur in intimate association with wittichenite in bismuth-bearing copper ores. In the experiments at 420°C, although wittichenite coexists with bornite solid solution, it is not found in the assem-

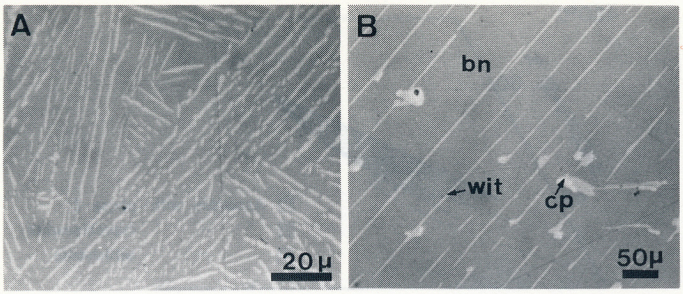

FIG. 19 A and B. Photomicrographs of exsolution lamellae of wittichenite in bornite. A, Wittichenite lamellae appeared in bornite in which produced at 420°C after annealed at 300°C; B, Wittichenite lamellae in bornite from the Sannotake-Yokozuru mine.

blage with chalcopyrite because the assemblages of bornite + cuprobismutite + nukundamite (or bismuth liquid) and bornite + phase $Cu_{8.4}Fe_{1.2}Bi_{10.8}S_{22}$ + nukundamite (or bismuth liquid) form in an equilibrium state. However, wittichenite appears in equilibrium with chalcopyrite in the experimental runs at 300°C. SUGAKI *et al.* (1972b) carried out the study on the phase relation in the pseudo-binary $CuFeS_2$–Cu_3BiS_3 using an evacuated glass tube method and found that the assemblage of chalcopyrite and wittichenite is stable below 395°C. Their result does not conflict with that of the experiments by the present authors. From these data, the chalcopyrite and wittichenite assemblage found in natural ores is interpreted to have been formed at temperatures below 395°C.

4.3 *Emplectite, chalcopyrite and bornite assemblage*

Although emplectite often occurs in intimate association with chalcopyrite and bornite in bismuth and copper ores, the assemblages of emplectite, chalcopyrite and/or bornite are not found in the experimental runs at 300°C because the assemblages of wittichenite, phase $Cu_{8.4}Fe_{1.2}Bi_{10.8}S_{22}$, and phase $Cu_8Bi_8S_{19}$ or bismuth liquid are stable, as shown in Fig. 15. It is not certain wherther the emplectite, chalcopyrite and/or bornite assemblages form at lower temperatures than 300°C or not, but it is possible that they appear as a stable association below 300°C. Also, in natural ores, emplectite commonly coexists with wittichenite, bismuthinite, and native bismuth. Among them, the assemblage of emplectite, wittichenite, and bismuth (liquid) occurs in the experiments at 300°C, but the association of emplectite and bismuthinite is not found. SUGAKI *et al.* (1980) reported from their experimental data that emplectite forms in association with bismuthinite at temperatures below approximately 280°C because of the decomposition of phase $CuBi_3S_5$ at that temperature, as shown in Fig. 7. Therefore, the emplectite and bismuthinite assemblage found in ores seems to have been formed at lower temperatures

than about 280°C. SUGAKI *et al.* (1980) also carried out the study on the relation between emplectite and cuprobismutite in the join Cu_2S–Bi_2S_3 as already mentioned, and found that cuprobismutite is more bismuth-rich than emplectite, which has stoichiometric composition $CuBiS_2$ and becomes unstable as to decomposed into emplectite and phase $CuBi_3S_5$ at 318°C or below. So cuprobismutite should not occur in nature, but it sometimes appears in ores. For this reason, it is thought that minor elements such as iron, lead, and silver contained in cuprobismutite may act as a stabilizer to keep cuprobismutite at room temperature.

4.4 Phase assemblages with bismuth

As bismuth minerals in natural ores, native bismuth is common as well as bismuthinite. In the present experiments of the system Cu–Fe–Bi–S at 300° and 420°C, bismuth (liquid) appears in company with all solid phases, except phase $Cu_8Bi_8S_{19}$, pyrite, covellite, and nukundamite, under the condition of relatively low sulfur fugacity, as seen in Figs. 13-B and 16-B. The tie lines from most of the sulfide phases in the quaternary space are concentrated upon a bismuth corner of the tetrahedron Cu–Fe–Bi–S. It means that almost all phases in the system can coexist as stable assemblages with bismuth under low sulfur fugacity. SUGAKI *et al.* (1972b) and NANRI *et al.* (1978) investigated phase relations in the Cu–Fe–Bi–S system under low sulfur fugacity by the dry method using an evacuated glass tube and obtained the results that bismuth (liquid) appears as a stable phase in all of the phase assemblages at 400°C. These results are in good agreement with those obtained under hydrothermal conditions by the present study. On the other hand, in the case of relatively-high sulfur fugacity, the tie lines are connected to phase $Cu_8Bi_8S_{19}$ (Y) and nukundamite instead of bismuth, as shown in Figs. 13-A and 16-A, and bismuth is not found.

4.5 Relation between phase $Cu_{8.4}Fe_{1.2}Bi_{10.8}S_{22}$ (Z) and hodrushite.

Phase Z is the only four-element compound in the Cu–Fe–Bi–S system synthesized by both the dry and hydrothermal methods. It occurs in a stable state at temperatures below 600°C. KODĚRA *et al.* (1970) found a new sulfosalt mineral, hodrushite $Cu_{8.12}Fe_{0.29}Bi_{11.54}S_{22}$, from Banska Hodoruša, Czechoslovakia. Hodorushite has a similar composition to that of phase Z. Its symmetry is monoclinic, space group $A2/m$, lattice constants $a = 27.21$ Å, $b = 3.39$ Å, $c = 17.58$ Å, and $\beta = 92.9°$. However, phase Z is monoclinic, $C2/m$, $a = 17.483$ Å, $b = 3.902$ Å, $c = 12.869$ Å, and $\beta = 108.11°$. Therefore, it is thought that phase Z is a different compound from hodorushite and has not yet been found in nature. Phase Z is stable at low temperatures and does not change, even after being kept in an evacuated glass tube for about 10 years at room temperature. Therefore, it is possible that phase Z will be found as a new mineral in nature.

A part of the expense for this study was defrayed by Grant in Aid for Scientific Research from the Ministry of Education of Japan. The writers offer their sincere thanks to the Ministry of Education.

REFERENCES

BARNARD, W. M. and CHRISTOPHER, P. A. (1966): Hydrothermal synthesis of chalcopyrite, *Econ. Geol.*, **61**, 897–902.

BARTON, P. B. (1973): Solid solutions in the system Cu–Fe–S, Part I: The Cu–S and CuFe–S join, *Econ. Geol.*, **68**, 455–465.

BARTON, P. B. and SKINNER, B. J. (1967): Sulfide mineral stabilities, in *Geochemistry of Hydothermal Ore Deposits*, Ed., H. L. Barnes, Holt. Reinhart and Winston, New York, pp. 236–333.

BENCE, A. E. and ALBEE, A. L. (1968): Empirical correction factors for the electron microanalysis of silicate and oxides, *J. Geol.*, **76**, 382–403.

BRETT, P. R. (1963): The Cu–Fe–S system, *Carnegie Inst. Wash. Year Book*, **62**, 1963–1966.

BRYSTOV, L. V. and KUZ'MINA, I. P. (1959): *Growth of crystals*, Vol. 3, Consultants Bureau, New York, p. 357.

BUHLMANN, E. (1971): Untersuchungen im System Bi_2S_3–Cu_2S und geologische Schlussfolgerungen, *Neu. Jahrb. Miner., Monat.*, **3**, 137–141.

CABRI, L. J. (1967): A new copper-iron sulfide, *Econ. Geol.*, **62**, 910–925.

CABRI, L. J. (1973): New data on phase relations in the Cu–Fe–S system, *Econ. Geol.*, **68**, 443–454.

CABRI, L. J. and HALL, S. R. (1971): Phase relations in the chalcopyrite region of the Cu–Fe–S system (abstr.), *Can. Mineral.*, **11**, 569.

CABRI, L. J. and HALL, S. R. (1972): Mooihoekite and haycockite, two new copper-iron sulfides, and their relationship to chalcopyrite and talnakhite, *Am. Mineral.*, **57**, 689–708.

CABRI, L. J. and HARRIS, D. C. (1971): New compositional data on talnakhite, *Econ. Geol.*, **66**, 673–675.

CHEN, T. T. and CHANG, L. L. Y. (1974): Investigations in the system Ag_2S–Cu_2S–Bi_2S_3 and Ag_2S–Cu_2S–Sb_2S_3, *Can. Mineral.*, **12**, 404–410.

CHERNYSHEV, L. V., ANFILOGOV, V. N., PASTUSHKOVA, T. M. and SUTURINA, T. A. (1968): A study of the system Fe–Zn–S under hydrothermal conditions, *Geochem. Intern.*, **5**, 196–209.

CRAIG, J. R. and SCOTT, S. D. (1974): Sulfide phase equilibria, in *Sulfide Mineralogy, Min. Soc. Am. Short Course Notes*, **1**, CS1–110.

CRAIG, J. R., BARTON, P. B. and SEPNUK, B. H. (1971): Experimental investigation in the Bi–Fe–S system (abstr.), *Geol. Soc. Am. Abstr. Prog.*, **3**, 305.

DANA, E. S. (1892): *Dana's System of Mineralogy*, John Wiley and Sons, New York, pp. 110–111.

FEDROVA, ZH. N. (1972): Investigation of phase digram of the Cu_2S–Bi_2S_3 system, in *Exp. Invest. in Mineralogy, 1970–1971*, Acad. Sci. USSR., Siber. Div., Inst. Geol. Geophy., Nobosibirsk, pp. 24–30 (in Russian).

GAUDIN, A. M. and DICKE, G. (1939): The pyrosynthesis, microscope study and irridescent filming of sulfide compounds of copper with arsenic, antimony and bismuth, *Econ. Geol.*, **34**, 214–230.

GODOVIKOV, A. A. and PTITSIN, A. B. (1969): Synthesis of copper-bismuth sulfosalts in hydrothermal conditions, in *Exp. Invest. in Mineralogy 1968–1969*, Acad. Sci. USSR., Siber. Div., Inst. Geol. Geophys., Novosibirsk, pp. 26–41 (in Russian).

GODOVIKOV, A. A., FEDOROVA, ZH. N., PAVLJUCHENKO, V. S. and PTITSIN, A. B. (1971): New

synthetic bismuth sulfosalt of copper–$Cu^{+1}Cu_2{}^{+2}Bi_3S_7$, in *Exp. Invest. in Mineralogy, 1969–1970*, Acad. Sci. USSR., Siber. Div., Inst. Geol. Geophy., Novosibirsk, pp. 3–9 (in Russian).

HILLEBRAND, W. F. (1884): Löllingite and other minerals, *Am. J. Sci.*, **27**, 355.

IKORNIKOVA, N. YU. (1962): The role of chlorides in the hydrothermal transportation of metals during the mineralization process (abstr.), *Econ. Geol.*, **58**, 1011.

KODERA, M., KUPCIK, V. and MAKOVICKY, E. (1970): Hodrushite—a new sulfosalt, *Mineral. Mag.*, **37**, 641–648.

KRIEGER, P. (1940): Bornite-klaprotholite relations at Concepcion del Oro, Mexico, *Econ. Geol.*, **35**, 687–697.

KULLERUD, G. (1953): The FeS–ZnS system, a geological thermometer, *Norsk Geol. Tiddsskr.*, **32**, 61–147.

KULLERUD, G. (1971): Experimental techniques in dry sulfide research, in *Research Techniques for High Pressure and High Temperature*, Ed. G. C. Ulmer, Springer, New York, pp. 288–315.

KULLERUD, G., YUND, R. A. and MOH, G. H. (1969): Phase relations in the Cu–Fe–S, Cu–Ni–S and Fe–Ni–S system, *Econ. Geol., Monogr. Ser.*, **4**, (magmatic ore deposits), 323–343.

KUZ'MINA, I. P. (1961): Experimental study of PbS and ZnS formation from aqueous solution of chlorides (abstr.), *Econ. Geol.*, **57**, 990–991.

LAUDISE, R. A., KOLB, E. D. and DENEUFVILLE, J. P. (1965): Hydrothermal solubility and growth of sphalerite, *Am. Mineral.*, **50**, 382–391.

MERWIN, H. E. and LOMBARD, R. H. (1937): The system Cu–Fe–S, *Econ. Geol.*, **32**, 203–284.

MUKAIYAMA, H. and IZAWA, E. (1970): Phase relations in the Cu–Fe–S system, the copper-deficient part, in *Volcanism and Ore Genesis*, Ed. T. Tatsumi, Univ. Tokyo Press, Tokyo, pp. 339–355.

NANRI, H., SUGAKI, A., SHIMA, H. and KITAKAZE, A. (1978): Phase relations of Cu–Fe–Bi–S system (V)—bornite solid solution field at 400°C and 500°C (abstr.), *J. Japan. Assoc. Mineral. Petrol, Econ. Geol.*, **73**, 83 (in Japanese).

NUFFIELD, E. W. (1947): Studies of mineral sulphosalts: XI—wittichenite (klaprothite), *Econ. Geol.*, **42**, 147–160.

NUFFIELD, E. W. (1952): Studies of mineral sulphosalts: XVI—cuprobismutite, *Am. Mineral.*, **37**, 447–452.

PALACHE, C. (1940): Cuprobismutite—a mixture, *Am. Mineral.*, **25**, 611–613.

PTITSIN, A. B. and GODOVIKOV, A. A. (1971): Hydrothermal synthesis of bismuth sulfosalts of copper in acid solutions and oxidative medium, in *Exp. Invest. in Mineralogy 1969–1970*, Acad. Sci. USSR., Siber. Div., Inst. Geol. Geophys., Novosibirsk, pp. 52–60 (in Russian).

ROSEBOOM, E. H. and KULLERUD, G. (1958): The solidus in the system Cu–Fe–S between 400°C and 800°C, *Carnegie Inst. Washington Year Book*, **57**, 222–227.

SCHLEGEL, H. and SCHÜLLER, A. (1952): Die Schmelz- und Kristallisations-gleischgewichte im System Cu–Fe–S und ihre Bedeutung für Kupfergewinnug, *Freiberger Forschung, sec. B*, 1–32.

SCHNEIDERHÖHN, H. and RAMDOHR, P. (1931): *Lehrbuch der Erzmikroskopie* Bd. 2, Berlin, pp. 378–379.

SCOTT, S. D. (1974): Experimental methods in sulfide synthesis, in *Sulfide Mineralogy, Min. Soc. Am. Short Course Notes*, **1**, S1–S38.

SCOTT, S. D. (1975): Hydrothermal synthesis of refractory sulfide minerals, *Fortschr. Mineral.*, **52**, 185–195.

SCOTT, S. D. and BARNES, H. L. (1971): Sphalerite geothermometry and geobarometry, *Econ. Geol.*, **66**, 653–669.

SHIMA, H., SUGAKI, A. and KITAKAZE, A. (1977): Phase equilibrium study in the Fe–Bi–S

system—synthetic phase $FeBi_4S_7$, *Abstr. Ann. Meet. Mineral. Soc. Japan*, p. 128 (in Japanese).

Short, M. N. (1931): Microscopic determination of the ore minerals, *U.S. Geol. Survery Bull.*, **914**, U.S. Geol Survery, Washington.

Sugaki, A. and Kitakaze, A. (1972): Chemical composition of synthetic alabandite solid solution and its phase relations in the system Mn–Fe–S, in *Proc. 6'th Intern. Conf. X-ray Optics and microanalysis, Osaka*, pp. 755–761.

Sugaki, A. and Shima, H. (1965a): Synthetic sulfide minerals (I), *Mem. Fac. Eng. Yamaguchi Univ.*, **15**, 15–31.

Sugaki, A. and Shima, H. (1965b): Synthetic sulfide minerals (II), *Mem. Fac. Eng. Yamaguchi Univ.*, **15**, 33–47.

Sugaki, A. and Shima, H. (1971): The phase equilibrium study of the Cu–Bi–S system, in *Proc. IMA–IAGOD Meeting '70, IMA Vol. Spec. Pap. No. 1, Tokyo.*, pp. 270–271.

Sugaki, A. and Shima, H. (1972): Phase relations of the Cu_2S–Bi_2S_3 system, *Tech. Rept. Yamaguchi Univ.*, **1**, 45–70.

Sugaki, A., Shima, H. and Nomiyama, S. (1970): Phase equilibrium study in the Fe–Bi–S system (abstr.), *J. Mineral. Soc. Japan.*, **10**, 110–111 (in Japanese).

Sugaki, A., Shima, H. and Kitakaze, A. (1972a): Synthetic sulfide minerals (IV), *Tech. Rept. Yamaguchi Univ.*, **1**, 71–85.

Sugaki, A., Kitakaze, A. and Yamamoto, T. (1972b): Phase equilibrium study of the Cu–Fe–Bi–S system (II)—wittichenite-chalcopyrite (abstr.), *J. Japan. Assoc. Mineral. Petrol. Econ. Geol.*, **65**, 105 (in Japanese).

Sugaki, A., Shima, H. and Kitakaze, A. (1973): Chemical composition and phase relations of naturally occurring Cu–Fe sulfides (abstr.), *Mining Geol. Japan.*, **23**, 61 (in Japanese).

Sugaki, A., Shima, H. and Kitakaze, A. (1974): Fundamental study on the quantitative analysis of sulfide minerals by electron probe microanalyser (V), *Mem. Fac. Eng. Yamaguchi Univ.*, **24**, 225–230 (in Japanese).

Sugaki, A., Shima, H., Kikakaze, A. and Harada, H. (1975): Isothermal phase relations in the system Cu–Fe–S under hydrothermal conditions at 350°C and 300°C, *Econ. Geol.*, **70**, 806–823.

Sugaki, A., Shima, H. and Kitakaze, A. (1976a): Hydrothermal synthesis of sulfide minerals with complex compositions, *Sci. Rept. Tohoku Univ., Ser. 3*, **13**, 115–129.

Sugaki, A., Shima, H. and Kitakaze, A. (1976b): Application of Bence and Albee method to analyses of sulfide minerals; Cu–Fe–Pb–Bi–S system, *J. Mineral. Soc. Japan*, **12**, Spec. Issue, 85–92 (in Japanese).

Sugaki, A., Shima, H., Kitakaze, A. and Fukuoka, M. (1977): Hydrothermal synthesis of pyrrhotite and their phase relations at low temperature, *Sci. Rept. Tohoku Univ., Ser. 3*, **13**, 165–182.

Sugaki, A., Shima, H. and Kitakaze, A. (1980): The phase equilibrium of the system Cu–Bi–S below 400°C, especially the relation between emplectite and cuprobismutite, in *Proc. 9'th IMA Meeting 1978*, sulphosalts, plutinum minerals and ore microscopy volume, pp. 100–109.

Sugaki, A., Shima. H., Kitakaze, A. and Mizota, T. (1981a): Hydrothermal synthesis of nukundamite and its crystal structure, *Am. Mineral.*, **66**, 398–402.

Sugaki, A., Kitakaze, A. and Hayashi, K. (1981b): Synthesis of minerals in the Cu–Fe–Bi–S system under hydrothermal condition and their phase relation, *Bull. Mineral.* **104**, 484–495.

Sugaki, A., Kitakaze, A. and Ueno, T. (1982): Hydrothermal synthesis of minerals in the system Cu–Fe–S and their phase equilibrium at 400°C and 500°C, *J. Japan. Assoc. Mineral. Petrol. Econ. Geol., Special Issue*, **3**, 257–269 (in Japanese).

Taylor, C. M., Radtke, A. S. and Christ, C. L. (1973): New data on cuprobismutite, *J. Res. U.S. Geol. Survey*, **1**, 99–103.

YUND, R. A. (1963): Crystal data for synthetic $Cu_{5.5x}Fe_xS_{6.5x}$ (idaite), *Am. Mineral.*, **48**, 672–676.

YUND, R. A. and KULLERUD, G. (1966): Thermal stability of assemblages in the Cu–Fe–S system, *J. Petrol.*, **7**, 454–488.

WATANABE, M. (1937): Geology and ore deposits of the Obari and Hongo mines, Yamagata Prefecture, Japan; especially mineral paragenesis of copper and copper-bismuth sulfides, *J. Japan. Assoc. Mineral. Petrol. Econ. Geol.*, **18**, 211–269; **19**, 27–32, 70–88 (in Japanese).

WATANABE, M. (1951): Lattice and graphic intergrowth of some copper minerals from the Obari mine, Japan, *Sci. Rept. Tohoku Univ., Ser. 3*, **4**, 1–10.